UNIVERSIDAD
NACIONAL
DE COLOMBIA

Sedimentary Facies distribution Impact on Heavy Oil Production in a Llanos Basin Field, Eastern Colombia

"Impacto de la Distribución de las Facies Sedimentarias en la Producción de Crudo Pesado en un Campo de la Cuenca Llanos, Oriente de Colombia"

Ángela María Betancur Soto

Universidad Nacional de Colombia
Facultad de Minas, Departamento de ingeniería de Materiales y Química
Medellín, Colombia
2021

Sedimentary Facies distribution Impact on Heavy Oil Production in a Llanos Basin field, Eastern Colombia

Ángela María Betancur Soto

A Thesis submitted in partial fulfillment of the requirements for the Degree of Master of Science in Petroleum Engineer

Advisor:
PhD., Agustín Cardona Molina

Co-Advisor:
MSc., Zorel Gutiérrez Granados

Universidad Nacional de Colombia
Facultad de Minas, Departamento de ingeniería de Materiales y Química
Medellín, Colombia
2021

With all my love for God, my beautiful family, and my husband, they have never given up on me, supporting and inspiring me to pursue my dreams.

I thank them for everything they have done for me.

Ángela María Betancur Soto.

The most beautiful sensation of victory
is when you overcome your fears.
Ángela

ACKNOWLEDGEMENTS

First, I would like to express my deepest appreciation to my thesis advisor and co-advisor Agustín Cardona of the Minas Faculty at National University, and Zorel Gutierrez of Ecopetrol S.A. They were always available with the best attitude to advise and answer technical questions. Many thanks for the consistent support and guidance during this project.

I would like to thank to Pedro Nel Benjumea Hernández who was the expert involved in the validation of this research project.

I'm extremely grateful to Jose Alberto Villasmil and Ecopetrol S.A. for providing the information involved in this study.

I must to extend my gratitude to Carlos Germán Herrera, petroleum engineering who helps me to solve some challenges related to engineering aspects. I am grateful for his invaluable help.

Finally, I must express my deepest thankfulness to God and my family for their company during this process giving to me their constant support and encouragement throughout my years of study. This achievement would not have been possible without them.

Ángela María Betancur Soto

CONTENTS

ABSTRACT **11**
RESUMEN **12**
SUMMARY **13**
INTRODUCTION **15**
PROJECT OBJECTIVES **16**

1. SEDIMENTOLOGICAL, GEOSTATISTICAL AND ENGINEERING CONCEPTUAL FRAMEWOR .17
1.1.FACIES MODEL 17
1.2.GEOSTATISTICAL MODEL 18
1.2.1. Spatial Correlation Analysis 19
1.2.2. Simulation 20
1.2.3. 3D Facies and Property Modelling Methods 21
1.3.HEAVY OIL 27
1.4.RELATIVE PERMEABILITY 27
1.4.1. Laboratory Water Oil Relative Permeability 28
1.4.2. Corey Correlation Water - Oil System 29
1.4.3. Heavy Oil Relative Permeability 29
1.5.PRESSURE BUILD UP 30
1.6.OIL RATE CALCULATION 32
1.7.PRODUCTIVITY INDEX 33

2. AREA OF INTEREST: MAIN CHARACTERISTICS 34
2.1.STUDY AREA LOCATION 34
2.2. REGIONAL GEOLOGY 35
2.3. LOCAL GEOLOGY 36
2.3.1. Local Stratigraphy 36
2.3.2. Local Structural Geology 37
2.4. SEDIMENTOLOGICAL MODEL 38
2.4.1. Well Tops Interpretation 39
2.4.2. Core Analysis 39
2.4.3. Depositional Environment Association 41
2.4.4. Facies Distribution Maps by Zones 42
2.5. PETROPHYSICAL MODEL 47
2.5.1. Shale Volume Model 48
2.5.2. Porosity Model 49

2.5.3. Permeability Model 49
2.5.4. Rock Type Model from Logs 49
2.5.5. Water Saturation Model 51
2.6. RESERVOIR ENGINEERING ASPECTS 51
2.6.1. Reservoir Pressure 51
2.6.2. Fluid Properties 52
2.6.3. Laboratory Water – Oil Relative Permeabilities 52

3. METHODOLOGY AND WORKFLOW 54
3.1.LITERATURE REVIEW 54
3.2. DATA PREPARATION 54
3.2.1. Information Gathering and Inventory 54
3.2.2. Data Quality Control 54
3.2.3. Lithofacies Inputs 55
3.3. 3D STATIC MODELLING 55
3.3.1. Building a 3D Grid 55
3.3.2. 3D Lithofacies Modelling 56
3.3.3. Petrophysical Modelling 56
3.3.4. Volumetric Calculation 56
3.3.5. Lithofacies Uncertainty Analysis 56
3.4. RESERVOIR ENGINEERING CALCULATIONS 57
3.4.1. Pressure Transient Analysis 57
3.4.2. Flow Capacity Match 57
3.4.3. Productivity Index 57
3.4.4. Calculation of Initial Oil Rate into Geological Grid 58
3.5. RESULTS AND CONCLUSIONS 58

4. RESULTS 59
4.1. STATIC 3D RESERVOIR MODELLING 59
4.1.1. 3D Model Description 59
4.1.2. Structural Framework 60
4.1.3. Lithofacies Curve Creation 62
4.1.4. Well Log Upscaling 66
4.1.5. Data Analysis 67
4.1.6. Data Distribution 70
4.1.7.3D Lithofacies Modelling 70
4.1.8. 3D Petrophysical Modelling 83

4.1.9. Volumetric Calculation 94
4.1.10. Lithofacies Uncertainty Analysis 94
4.2. ENGINEERING CALCULATION AND ANALYSIS 97
4.2.1. Oil Relative Permeability Proposed Correlation 97
4.2.2. Oil Rate Match per Well Using the Proposed Heavy Oil Relative Permeability 99
4.2.3.Pressure Transient Analysis of Vertical Wells 100
4.2.4.Initial Oil Rate in 3D Static Model Grid 102

5. DISCUSION 106
5.1.FACIES MODEL DISTRIBUTION PREDICTABILITY 106
5.1.1.Blind Test 106
5.1.2.Predicitability among Modelling Techniques 113
5.2.Facies Distribution Impact on Initial Oil Rate in a Heavy Oil Reservoir 115
5.2.1. Facies Distribution Impact an the Initial Oil Rate Production in A Heavy Oil Field 115
5.2.2. Retarding Rock 121
5.3. SWEET SPOTS WITH DIFFERENT FACIES DISTRIBUTION MODELS 122
5.3.1. GEOLOGICAL APPROACH 122
5.3.2. ENGINEERING APPROACH 123
5.3.3. SWEET SPOT TECHNIQUES COMPARISON 124

6. CONCLUSIONS 127
RECOMMENDATIONS 129
REFERENCES 130

APPENDICE 134
APPENDIX A. Vertical Proportional Curves 134
APPENDIX B. Facies Variograms 136
APPENDIX C. Lithofacies And Sedimentological Maps 149
APPENDIX D. Probability Lithofacies Trend Modeling 150
APPENDIX E. Lithofacies Model And Property Model 152
APPENDIX F. Histograms Stoiip 300 Realizations. Training And Base Cases For All Models 156
APPENDIX G. Lithofacies Model All Percentiles By All Methods Modeled Layer 19 Zone 2 157
APPENDIX H. PI Cumulative Maps All Percentiles By All Lithofacies Methods Modeled 158
APPENDIX I. Oil Rate Cumulative Maps All Percentiles By All Lithofacies Methods Modeled 159
APPENDIX J. Example Transition Lithofacies Zone (Retarding Rock And Reservoir Rock) WELL W-568 160

FIGURES LIST

Figure 1-1. Environmental interpretation of gamma ray response (adapted from Cant, D.J. 1992) and electrofacies map zone B, AOI (adapted from Navas, 2016)……18
Figure 1-2. Classical parameters of the variogram (adapted from Barca, E., Bruno, et al 2016)……20
Figure 1-3. Procedure of truncated gaussian simulation on the left hand and indicator transform on the right hand (adapted from Bahar, A. 2014)……...22
Figure 1-4. Procedure of multiple point simulation (adapted from Schlumberger, 2011)……..24
Figure 1-5. Monte Carlo general process 3D static model uncertainty……..26
Figure 1-6. a. Representation of relative permeability curves. b. Simple sketch of relative permeability lab procedure…..28
Figure 1-7. PBU test in W-091 that belongs to AOI……30
Figure 1-8. PBU conceptual model……..31
Figure 1-9. Ideal behavior of pressure derivative……..31
Figure 2-1. Area of interest location……34
Figure 2-2. Regional stratigraphy chart (adapted from Alfaro, C & Alvarado, I. 2014)……..35
Figure 2-3. Local stratigraphic column……37
Figure 2-4. Structural surface from well tops to Carbonera C7 zone B……38
Figure 2-5. Squematic cross section of area of interest……39
Figure 2-6. Core and samples in the zone of interest and sedimentological description well W-158 (adapted from Ramirez, 2010)……...41
Figure 2-7. Thickness of the environments interpreted in Carbonera C7 found in W-158……42
Figure 2-8. Sedimentological description of zone D well W-158……..44
Figure 2-9. a. Electrofacies maps zone A and well correlation. b. Electrofacies maps zone B and well correlation……45
Figure 2-10. a. Electrofacies maps zone C and well correlation. b. Electrofacies maps zone D and well correlation…….46
Figure 2-11. Lithotypes used in the petrophysical model……..48
Figure 2-12. a. Pore throat radius by rock type, b. capillary pressure by rock type and c. Pitman R50 graph. (Modified from Ecopetrol, 2017)……50
Figure 2-13. a. Reservoir pressure map. b. Oil viscosity map……52
Figure 2-14. Relative permeability curves by rock type……53
Figure 3-1. General workflow - Methodology……...58
Figure 4-1. Relation between numbers of wells by perforated zones……59
Figure 4-2. 3D static model workflow……..60
Figure 4-3. 3D geostatistical lithofacies modelling methods……..60
Figure 4-4. Zones configuration……...61
Figure 4-5. Representation of layering defined……62
Figure 4-6. Normalized gamma ray cut-off……..63
Figure 4-7. Crossplot lithofacies versus porosity and permeability versus lithofacies……63
Figure 4-8. Example of initial lithofacies and simplified lithofacies……..65
Figure 4-9. Crossplot permeability versus porosity versus lithofacies……65
Figure 4-10. Well logs vs upscaled logs lithofacies, Vshale, porosity and permeability histogram……66
Figure 4-11. Anisotropy and electrofacies maps by zone……..68
Figure 4-12. Workflow to build 3D facies and petrophysic probabilistic scenarios models……72
Figure 4-13. Histogram for sequential indicator simulation (SIS) base case: Using facies preferential direction tendency. SIS model percentile P50……73
Figure 4-14. Example of lithofacies base case and P50 at zone 2 layer 19……74
Figure 4-15. Electrofacies grouped by regions……..75
Figure 4-16. Histogram SIS Hierarchy Geomorphologic from electrofacies maps as a hard data for all percentiles modeled……..76
Figure 4-17. SIS Hierarchy geomorphologic lithofacies Example, for all percentiles modeled in zone 2 layer 19……77
Figure 4-18. Histogram lithofacies model by Truncated Gaussian Simulation (TGS)……78
Figure 4-19. Example of lithofacies model by TGS, layer 19 zone 2……..78
Figure 4-20. General information about images selected to control the lithofacies model……..79
Figure 4-21. Process and results multiple point simulation and some examples……80
Figure 4-22. Histogram lithofacies model by Multiple point Simulation (MPS)……..81
Figure 4-23. 3D Facies distribution zones 1, 2, 3, and 4 by MPS percentiles P10, P50 and P90……..82
Figure 4-24. 3D Facies distribution zones 5, 6 and 7 by MPS percentiles P10, P50 and P90……83
Figure 4-25. Porosity histograms……85

Figure 4-26. Permeability histograms……...85
Figure 4-27. Porosity vs permeability crossplot filtered by lithofacies scenario P50 for all methods modeled……86
Figure 4-28. Example of lithofacies influence on porosity and permeability distribution, zone 2 layer 19 for all lithofacies model percentile P50……...87
Figure 4-29. Shale volume and net to gross histograms for percentile P50……88
Figure 4-30. Example of lithofacies influence on NTG distribution, zone 2 layer 19 all lithofacies P50 methods.....…...89
Figure 4-31. Porosity and permeability crossplot - SIS facies model…….…….....90
Figure 4-32. Example of lithofacies influence on rock type distribution, zone 2 layer 19 all lithofacies modeled P50……91
Figure 4-33. 3D water saturation distribution NWW-SE direction……92
Figure 4-34. Example of lithofacies influence on water saturation distribution, zone 2 layer 19 all lithofacies methods modeled percentile P50……...93
Figure 4-35. Scenarios modeled to evaluate the sensitivity of major range and seed…….……95
Figure 4-36. Tornado graph……96
Figure 4-37. Histogram of STOIIP using 30 samples……...……97
Figure 4-38. Conceptual interpolated oil relative permeability……..98
Figure 4-39. End-points correlation with viscosity……...……99
Figure 4-40. Matched Initial oil rate and Final Interpolated oil relative permeability by tuning mo factor for rock type 1.100
Figure 4-41. Multilayer behavior W-091……101
Figure 4-42. Kh Static model vs pressure transient analysis (PTA)……...102
Figure 4-43. Oil rate calculation……103
Figure 4-44. Oil relative permeability calculated into the 3D grid (Zone2, Layer 19)……..……104
Figure 4-45. Calculation of interpolated oil relative permeability into the 3D grid (Zone2, Layer 19)……105
Figure 4-46. 3D initial oil rate Calculation (zone 2, layer 19)……105
Figure 5-1. Lithofacies model layer 19 zone 2, SIS all wells and SIS blind test P50……107
Figure 5-2. Well intersection to represent the blind wells model SIS P50……108
Figure 5-3. Lithofacies model layer 19 zone 2, Hierarchy geomorphologic all wells and blind test P50……..109
Figure 5-4. Well intersection Comparing well Lithofacies log and lithofacies model predicted under SIS hierarchy geomorphologic method P50……110
Figure 5-5. Lithofacies model layer 19 zone 2, TGS all wells and blind test P50……111
Figure 5-6. Well intersection Comparing well lithofacies log and lithofacies model predicted TGS P50……..…111
Figure 5-7. Lithofacies model layer 19 zone 2, MPS all wells and blind test P50……112
Figure 5-8. Well intersection comparing well lithofacies log and lithofacies model predicted under MPS method P50…..113
Figure 5-9. Accuracy among wells for lithofacies distribution methods P50……114
Figure 5-10. Precision among wells for lithofacies distribution methods P50……...114
Figure 5-11. Lithofacies distribution and oil rate grid at layer 19 zone 2……115
Figure 5-12. Predicted initial oil rate with the blind test model by wells and lithofacies method……116
Figure 5-13. Well intersection in the well W-568 SW-NE direction……117
Figure 5-14. Well intersection in the well W-091 SW-NE direction……118
Figure 5-15. Well intersection along the closest wells to the W-119……119
Figure 5-16. Relationship of facies predictability and oil production predictability……...120
Figure 5-17. Retarding Rock - Facies distribution impact on the initial oil rate production in a heavy oil field……121
Figure 5-18. Retarding rock - Facies distribution impact on oil rate production in a heavy oil field……..…...122
Figure 5-19. Range of possible sweet spots with different facies distribution models, by using geological approach (heat maps with Kroint) and comparison among Hydrocarbon pore volume maps……123
Figure 5-20. PI maps P50 percentile by lithofacies modeled methods……..124
Figure 5-21. Sweet spot comparison maps by lithofacies modeled methods percentile P50……..125
Figure 5-22. Crossplot average lithofacies versus initial oil rate production……126

TABLE LIST

Table 1. Main characteristics of pixel-based models……..……22
Table 2. Requirements for training image…….....24
Table 3. Main characteristics of property models methods……....25
Table 4. Crude oil classification by National Petroleum Agency of Brazil…….....27
Table 5. Parameter value used to calculate porosity from neutron -density log……49
Table 6. Parameter R50 value used to calculate rock types……50
Table 7. Description about rock types characteristic. (Modified from Ecopetrol, 2017)…….…..51
Table 8. Main fluid properties…….….52
Table 9. Laboratory relative permeability end-points……....53
Table 10. General grid properties……..……61
Table 11. Number of layers by zones…….…..62
Table 12. Azimuth and preferential direction used in variogram models…….…….68
Table 13. Vertical variogram search radius vs zone thickness…….……..69
Table 14. Results of variograms used to model facies through SIS using facies tendency preferential direction modelling……69
Table 15. Results of variograms used to model facies through SIS hierarchy geomorphologic method in the trend modelling……70
Table 16. Summary of probability cubes by lithofacies results……...76
Table 17. Statistic report of porosity for modeled and upscaled logs……..84
Table 18. Statistic report of permeability for modeled and upscaled logs……...84
Table 19. Volumetric report of base cases percentile P50……..94
Table 20. Parameters used in the sensibility evaluation……..95
Table 21. PBU main parameters…….101

ABSTRACT

Historically, lithofacies modeling and its uncertainty has been Aquila's ankle in achieving reservoir model objectives, as the uncertainty generally is evaluated through variogram sensitivity. Throughout this thesis a new workflow will focused on capturing lithofacies uncertainty and assess its impact on heavy oil production. The workflow combines static and dynamic properties into the three-dimensional grid without performing a dynamic simulation process.

Seed is the starting point of a random number generator for geostatistical simulation. In disciplines outside of oil and gas industry this is well understood and researched. However, during geological modeling seeds are fixed as an input parameter, which ignore the effect on unsampled areas. The new proposed methodology assesses the impact of seed number on lithofacies uncertainty distribution.

In the dynamic section, the thesis focus on the applicability of Darcy equation to QC the static model and proposed a modified heavy oil relative permeability correlation to calculate oil rate directly from static model. 1D analysis shows excellent results in vertical wells which gives confidence on static model. A 3D blind test of the integrated workflow shows precision of the lithofacies and potential oil rate prediction ranging between 50 and 80 % within the ±1 foot window.

The results show the importance of seed input on the distribution of properties in unsampled areas, which has been ignored for decades, on reducing the uncertainty on lithofacies distribution which has significant impact on STOIIP, hydrocarbon productivity and sweet spots identification. By including the modified oil relative permeability correlation in the static reservoir modeling workflow, a geomodeler can highlight prospective oil areas (sweet spots) through heat maps. This novel methodology can be implemented to any static reservoir modeling project from dry gas up to heavy oil.

Key words: lithofacies, seed, uncertainty, random, heavy oil relative permeability correlation, predictability, precision.

RESUMEN

Históricamente, el modelamiento de las litofacies y su incertidumbre han sido el talón de Aquiles para lograr los objetivos del modelamiento de yacimientos, ya que la incertidumbre generalmente se evalúa a través de la sensibilidad del variograma. A lo largo de esta tesis, un nuevo flujo de trabajo se centrará en capturar la incertidumbre de las litofacies y evaluará su impacto en la producción de crudo pesado. El flujo de trabajo combina propiedades estáticas y dinámicas en la malla tridimensional sin realizar un proceso de simulación dinámica.

La semilla es el punto de partida de un generador de números aleatorios para la simulación geoestadística. En disciplinas fuera de la industria del petróleo y el gas, esta está bien entendida e investigada. Sin embargo, durante el modelamiento geológico, las semillas se fijan como un parámetro de entrada, que ignora el efecto en las áreas no muestreadas.

La nueva metodología propuesta evalúa el impacto de la semilla en la distribución de la incertidumbre de las litofacies. En la sección dinámica, la tesis se centra en la aplicabilidad de la ecuación de Darcy al control de calidad del modelo estático y se propone una correlación de permeabilidad relativa para petróleo pesado modificada para calcular la tasa de petróleo directamente a partir del modelo estático.

El análisis 1D muestra excelentes resultados en pozos verticales, lo que brinda confianza en el modelo estático. Una prueba ciega en el flujo de trabajo 3D integrado, muestra la precisión de la predicción de las litofacies y el potencial de la tasa de aceite, que varía entre el 50 y el 80% evaluado dentro de la ventana de ± 1 pie.

Los resultados muestran la importancia de la entrada de la semilla en la distribución de propiedades en áreas no muestreadas, la cual ha sido ignorada durante décadas, en la reducción de la incertidumbre en la distribución de litofacies que tiene un impacto significativo en STOIIP, productividad de hidrocarburos e identificación de zonas de hidrocarburo prospectivas. Al incluir la correlación de la permeabilidad relativa del petróleo modificado en el flujo de trabajo de modelamiento de yacimientos estáticos, un geomodelador puede resaltar las posibles áreas de petróleo (Sweet spots) a través de mapas de prospectividad de aceite. Esta nueva metodología se puede implementar en cualquier proyecto de modelamiento de yacimientos estáticos, desde gas seco hasta petróleo pesado.

Palabras claves: litofacies, semilla, incertidumbre, aleatorio, correlación de permeabilidad relativa para crudo pesado, predictibilidad, precisión.

SUMMARY

A sedimentological model evaluation is an important aspect to be included in the static model, mainly for reservoirs with stratigraphic trapping, because it guides and controls the properties distribution as both are part of the reservoir configuration. One of the major modelling challenges is to capture the facies distribution uncertainty associated to heterogeneity and their impact on oil production. Therefore, it is necessary to consider different equiprobable scenarios to capture the uncertainty and reduce the bias associated of the interpreter in unsampled areas.

Facies uncertainty can be represented by seed or variograms sensitivities. It in this study, it was investigated the Seed geostatistical parameter as it handles the started point of the facies simulation algorithm which is normally random selected. Few published studies exist that investigates the Seed impact on static model predictability.

The nature is random and to study the possible outcomes of unknown areas this study used seed as uncertainty parameter. Random numbers are a geostatistical simulation keystone as it a very sensitive variable to evaluate bodies distribution uncertainty.

Seed allows to study vertical and areal lithofacies distribution across all layers keeping the global lithofacies proportion and generates a variation around 15% in STOIIP among the models. 2400 seed sensitivity realizations were run in four models and they were represented by five selected percentiles where the bodies distribution was modified in unsampled areas while preserving global lithofacies proportion.

This research uses these static model realizations to study two approaches to identify sweet spots, one approach based on static variables cut offs while the second approach used the productivity index. Through these proposed methods is possible to recognize prospective areas, as a result was found the north area as in the modeled area the north west part was the clearest one.

Sequential indicator simulation (SIS) using sedimentological maps was the most accurate method. Its accuracy is because it uses the sedimentological maps as a second variable which controls directly the lithofacies model.

It was identified a better correlation of potential oil rate and lithofacies predictability for all P50 percentiles blind test methods the predictability obtained was over 60%.

The heavy oil viscosity highly depends on the temperature which directly impacts its mobility; these features affect directly the oil relative permeability. Being relative permeability a high impact variable into the oil rate calculation.

Several oil relative permeability correlations have been proposed in the literature to capture the oil viscosity effect on these curves. It was investigated in this study a new successful approach that simplifies some these correlations by using the adimensional oil viscosity and a parameter that helps to tune the oil relative permeability using oil production data from vertical wells.

This study provides new insights and a new workflow by including common dynamic analysis into static modelling. Oil rate and productivity Index calculations in the static model are a valuable quality control tool of the static model. History matching process highly depends on the initial inputs. If the initial oil rate is close to the observed data, the uncertainty analysis during the dynamic stage can focus on other parameters (for example: heterogeneities) instead of trying to match relative permeability curves.

Sweet Spots using productivity (PI) summarize all the work proposed in this study as they are the results of 1) the uncertainty in facies distribution, 2) the proposed geological workflow step using Darcy law, and 3) the proposed oil relative methodology that incorporates oil viscosity.

INTRODUCTION

The Eastern Llanos basin has different types of trapping mechanisms. The hydrocarbon accumulation in the western part of the basin is associated to structural trapping and the eastern part is linked to combined and stratigraphic traps. Specifically, the area of study is related mainly to stratigraphic trapping.

This project is developed in the eastern domain of Llanos basin with heavy oil of 12 API. The reservoir unit belongs to the bottom of Carbonera Formation and consists of sandstone with high permeability (up to 1.5 darcys).

Geological models and dynamic simulation models are part of the integral understanding of the reservoir. They are a graphical and numerical representation of the subsurface rock and fluids. All those models integrate tools used to define the development strategy of an oil field. These strategies may involve multiple activities such as: drilling new wells, workovers, enhanced oil recovery (EOR)/improved oil recovery (IOR) projects, opening new production zones and stimulation projects.

The representation of geological features and petrophysical properties are relevant to understand the reservoir as they control the fluids accumulation and flow behavior of fluids in the porous media. In Addition, those models can help to infer the properties of unsampled areas.

A reservoir with stratigraphic traps tends to have compartmentalization related to the presence of various storage units and seals, as well as preferential depositional direction, presence of main and secondary channels, different channels width, lateral and vertical facies association, etc. The sedimentologic model can explain all the details needed to determine the reservoir configuration and heterogeneity in the static model.

In the process of building a geologic model, it is important to understand and represent the sedimentary structure of different sedimentary rocks, keeping in mind their uncertainties. Therefore, it is recommended to use sedimentary models to create different scenes to support the interpolation of petrophysical properties. Even though petrophysical variables such as porosity and permeability are related to lithofacies characteristics, the uncertainty remains in unsampled areas (Cannon Steve, 2018).

The area selected has a high heterogeneity associated with areas of high uncertainty caused by the depositional environment. Fluvial and transitional environments, which were exposed to continuous depositional energy changes that affects the sediments supply in quantity and quality.

Facies uncertainty is highly associated to the heterogeneity, this aspect was mainly recognized in laminations found in the vertical column and areal changes in the reservoir zones. The integration of sedimentological heterogeneities to a small scale it is essential to improve the accuracy and reliability of static models and their volume calculations.

This project developed several facies distribution scenarios, starting from a base model interpreted by a sedimentologist. Three geostatistical methods are studied such as sequential indicator simulation (SIS), truncated gaussian function (TGS) and multiple point simulation

(MPS). A total of 2400 realizations were run, which helped to select the final base case. Finally, five cases corresponding to percentiles 10, 35, 50, 75 and 90 were selected and compared using the oil in place volume, in order to populate static property parameters and determine the impact on oil production. These equiprobable geo-cellular models were used to calculate cell by cell productivity index and oil rate.

Variograms, and vertical proportion curves were used to control the facies model. Then, seed parameter was used to generate different uncertainty cases with minimum 300 realizations. Additionally, other cases were created using seed sensitivity with the same number of realizations and one training image for each depositional environment present in the reservoir.

The predictability assessment of the different facies distribution models shows that the unsampled zones cannot predict the facies in a distance longer than 500 meters when a second attribute or variable to control the model is not included. When a second attribute is used as the background of the static model, it has more chances to predict of facies and properties of the unknown location.

When different facies models' percentiles are compared, they show variations in the oil rate depending on the proportions of sandstone. Therefore, it was found that the proportion of reservoir facies is not necessarily directly proportional to the oil rate, due to the presence of transitional lithofacies belonging to the limit between retarding rocks and reservoir rock which can be associated with rock type six (poor quality rock) being mainly saturated with water. Hence, reservoir rocks lithofacies predictability is not necessarily coincident with oil rate predictability. One example of this is the upper interval opened in well W-568.

Oil relative permeabilities is a sensitivity variable, which is affected if the oil viscosity changes in heavy oil. This study proposes an oil relative correlation to match the oil rate in vertical wells. This proposal uses the laboratory oil relative permeability information at different viscosities to correlate the data in unsampled areas.

The main goal of the reservoir model is to identify new hydrocarbon opportunities to be developed in future campaigns. This study applied some approaches to identify a sweet spot combining static and dynamic analysis.

PROJECT OBJECTIVES

General Objective

The main objective of this project is to study the impact of sedimentary facies on heavy oil production rate in a Llanos Basin field by using multiple facies realizations and calculating the initial oil rate into the static model grid.

Specific Objectives

1. Assess the predictability of different facies distribution models.
2. Quantify facies distribution impact on the initial oil rate production in a heavy oil field.
3. Identify a range of possible sweet spots by using different facies distribution models.

1. SEDIMENTOLOGICAL, GEOSTATISTICAL AND ENGINEERING CONCEPTUAL FRAMEWORK

This section introduces the main theoretical concepts developed in this research, such as: facies model, geostatistics, and reservoir engineering.

1.1. FACIES MODEL

A facies model is a general summary of the characteristics of a given depositional system. This summary is modeled and it acts as a rule for the purposes of comparison and interpretation. They provide a kind of "mental picture" of the properties of rocks deposited in each environment (Boggs S, 2006).

Sedimentologists who works for petroleum industry use core gamma ray and image logs as an elemental tool to build areal facies models.

Electro-facies are facies defined using a set of well-log responses that follow a lithologic characteristic and it is different ones to others. In the oil industry is common to use gamma ray log signature as predictors of facies (Isimbab O, 2018). Log data specifically gamma ray covers areas without core, which helps to complement the interpretation along the area of study.

Gamma ray (GR) log is related to lithological and grain size response. The GR response is associated with an electro-shape and it is correlated to a possible genetic source. The upper part of Figure 1-1 shows each gamma ray shape and its possible genetic interpretation.

Figure 1-1 is an example of electrofacies map, it represents the facies distribution along with the area of interest, and this figure correlated each gamma electro-shape with each body represented in the map. The numbers 1, 2, 3 and 4 represent the correlation between every electro-shape represented in the map as body areally connected. For example: cylindrical GR has number 1 and it is represented in the map by orange color. This electro-shape also shows the main channel distribution inside the area of interest (AOI).

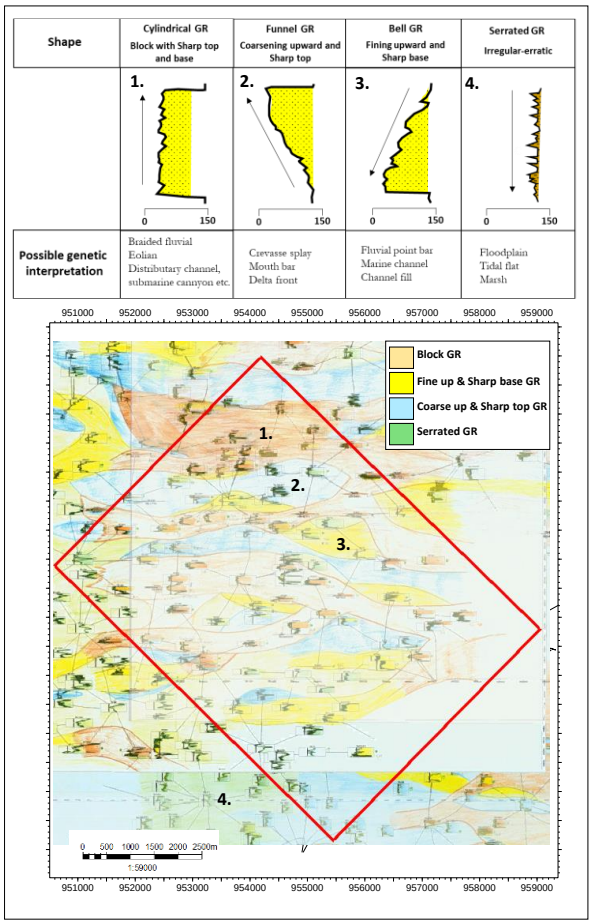

Figure 1-1. Environmental interpretation of gamma ray response (adapted from Cant, D.J. 1992) and electrofacies map zone B, AOI (adapted from Navas, 2016)

1.2. GEOSTATISTICAL MODEL

This discipline is a relatively new branch of statistics created for spatial analysis and uncertainty studies (Cannon Steve, 2018). The motivation to develop this tool was initially oriented to analyze data from gold-mining operations. Now, geostatistic techniques are implemented in many fields as a practical method of modelling a geologic phenomenon (Pyrcz & Deutsch, 2014)

Geostatistics tool used to model the reservoir heterogeneity into the static models. It offers strong methods for risk and uncertainty analysis in geological and dynamic modelling. Additionally, through this tool, it is possible to integrate several data sets collected at different scales (Cannon Steve, 2018).

The selection of proper application of geostatistical techniques for 3D modelling will result in reliable geological models to improve the understanding of reservoir dynamics (Cannon Steve, 2018).

1.2.1. Spatial Correlation Analysis

An important step of geostatistical modelling is to quantify the spatial correlation to estimate and simulate different variables. Each variable (facies, porosity, and permeability) in the reservoir has a different spatial variability.

The variogram is the most common method to quantify spatial correlation for any variable. Modelling and selection of the parameters to calculate the variogram is an important step to properly achieve an interpretable variogram.

The challenge encountered by the geomodeler is to calculate the experimental variogram. It is fundamental to define them in three directions and properly identify the nugget, sill, and lag distance. This is no easy task and requires sufficient high quality input data and geomodeler experience (Cannon Steve, 2018).

Variograms or **Semivariograms** are tools to analyze the spatial relationship of a variable in a defined area, the result is an experimental variogram which shows the maximum distance and the shape in one point and its influence on other points at different distances.

The variogram is defined as 2γ(h) is shown in Equation 1-1, it means: two times the variance multiplies by distance (h), in other words it is the variance of the increments of a regionalized variable in a location separated by a given distance (Journel & Huijbregts, 1978).

$$2\gamma(h) = var\big(Z(x+h) - Z(x)\big) \quad \textbf{Equation 1-1}$$

Where:

Var : Variance.
2γ (h) : Variogram.
h : Distance.
Z(x+h): Sampling value.
Z(x) : Values of the variable at position x.

Theoretical variogram can be divided in: delimited (linear, logarithm, and potential) and lying down (spherical, exponential and gaussian). The second group (lying down) guarantees infinite increments of covariance, which is why they are widely used to represent a good fit.

The parameters defined in each variogram are summarized in Figure 1-2.

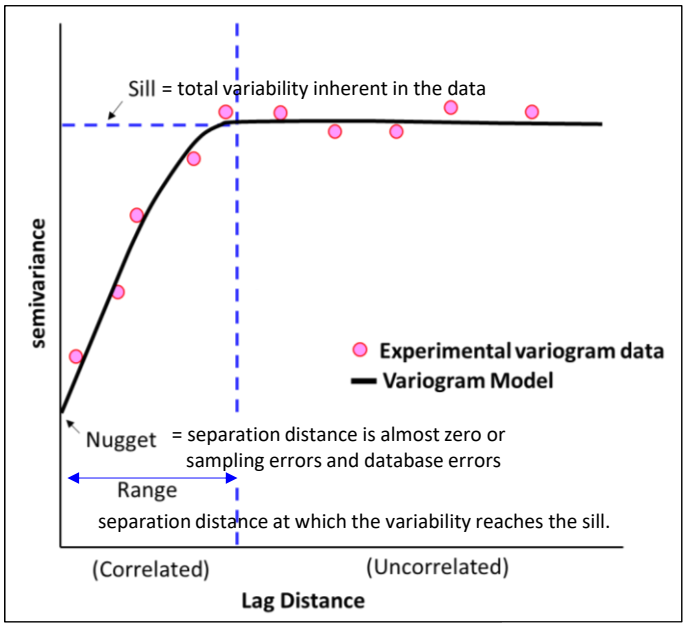

Figure 1-2. Classical parameters of the variogram (adapted from Barca, E., Bruno, et al 2016).

The variogram needs to be calculated in 3D and it is done by calculating 3 variograms: 1 vertical variogram, and 2 horizontal variograms (major and minor direction).

All variograms (major, minor, and vertical) use the same linear combination of models, they will have same nugget, sill, and the range can be different. The variogram is defined as an ellipsoid with three axes representing three different ranges.

(Cannon Steve, 2018), offers some recommendations to model a variogram, that can be used for discrete or continuous properties as a starting point:

- Select the domain to analyze and model (lithofacies or depositional system scale).
- Capture the main geological features which have a high impact.
- Detect short-scale variability, especially for continuous properties.
- Identify and remove bad data points which affect the variogram.
- Reduce lag distance, if it is possible and re-calculate variogram.
- For horizontal variograms, it is necessary the well spacing to be smaller than the actual length correlation.

1.2.2. Simulation

Simulation algorithms randomly sampled values from the conditional distribution at a specified point to estimate the property. The random constrain models the variance and reflects the spatial distributions. Each realization always honors the data and the variogram.

Simulation does a much better job (visually) to represent the data than kriging method; it guarantees to capture the variance and honors the data distribution. There are many simulation methods commonly used for property modelling such as sequential gaussian (SGS) and gaussian random function (GRFS).

Base on Cannon Steve, (2018) simulation reproduces the extremes of permeability and directional variability, whereas kriging only captures the directional variability. Capturing the degree of heterogeneity in permeability is very important because it controls the fluid flow through a porous media.

All simulation methods such as sequential indicator simulation, truncated gaussian simulation. Sequential gaussian simulation, and multiple point simulation, work under influence of the random number generator which stablish the order to visit the cells and populate them. The seed used is saved to re-built the way to populate models.

Testing random number generators has been wells study, nevertheless Ortiz & Deutsch (2000), suggest to carefully check the literature about this topic. They report different tests done to these generators which have been successful for certain periods, but then fail in new test processes.

1.2.3. 3D Facies and Property Modelling Methods

Modelling methods allow to represent the reservoir geometry and distribution. To build a model, it is necessary to use a geostatistic method which study the phenomena variation of geological properties by different techniques to describe spatial continuity[1].

3D static models use simulation techniques, the ability of these techniques consists of capturing the variance (or heterogeneity) of a spatial data distribution, this heterogeneity has an important effect on fluid flow, hence in the development of a field.

1.2.3.1. Facies Modelling Methods

The main goal to model facies is to capture the reservoir heterogeneity characterized by the sedimentary geology into the architecture of the geo-cellular grid. Facies model reflect an interpreted depositional model controlled by wells data (core, electrical logs) or seismic attribute data. It is possible to test the predicted proportion and distribution of any facies through the stochastic method to populate facies model

Pixel-based model is a geostatistical method based on the variogram as a measure of spatial variation or correlation of a property (Cannon Steve, 2018).

Some the most popular pixel-based methods are: Sequential indicator simulation, truncated Gaussian simulation and sequential Gaussian simulation. Each of them captures the uncertainty through multiple realizations. They allow to use trends or seismic attributes.

This method does not reproduce a specific geometry, but reproduces the lateral continuity and simulates realizations of a random function. Using variograms, a pixel-based method simulates values by grid node.

Table 1 shows the main aspects of pixel methods and their procedures to calculate the simulation.

[1] Mehrdad, S., & Behshad, J. (2015, January 29). 3D static reservoir modelling by geostatistical techniques used for reservoir characterization and data integration. Springer (Environmental Earth Science). doi:10.1007/s12665-015-4130-3

Pixel based methods		
Simulation Method	**Main Characteristics**	**Procedure to calculate**
Indicator	• Supported by indicator variograms and it uses simple kriging to calculate the probability of a facies transition. • Applicable when the density of well information is high and short wells distance. • Widely used for diagenetically controlled facies (Pyrcz & Deutsch, 2014). • Applied to different kind of depositional systems such as deep-marine "turbiditic" settings, deltaic, aeolian, and alluvial. • It is restricted to less continuous models	• Transform the original facies into the probability. • Perform variogram analysis for each facies. • Random path determination. • Estimate the probability for each facies using kriging. • Uncertainty quantification by combining probability for all facies. • **Back transformation by random sampling.**
Truncated Gaussian (TGS)	• Commonly used to model transitional facies. • It applies a Gaussian field, and then truncates it into discrete facies. • The sampling is based on sequential gaussian simulation (SGS) instead of random sampling.	• Organization of ordered lithotypes. • Perform variogram analysis. • Estimate the probability for each facies Ordinary kriging. • Facies estimation in gaussian domain. • Cumulative normal score calculation.

Table 1. Main characteristics of pixel-based models.

Figure 1-3 shows graphically the procedure for indicator and truncated gaussian simulation.

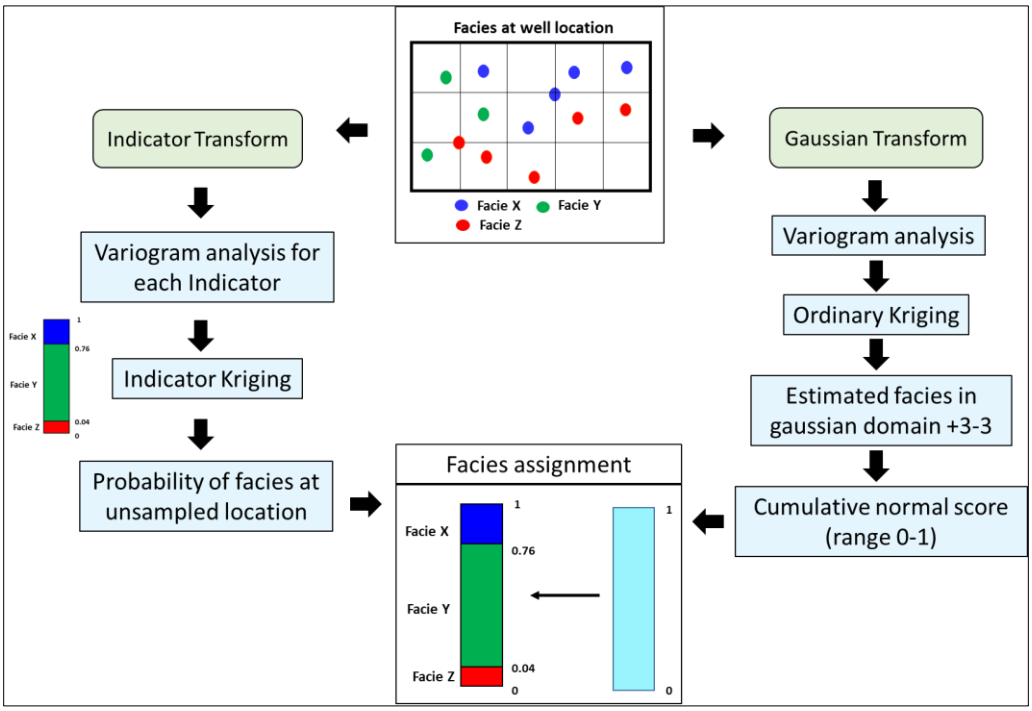

Figure 1-3. Procedure of truncated gaussian simulation on the left hand and indicator transform on the right hand (adapted from Bahar, A. 2014).

Multiple Point Statistic (MPS)

Multiple-point geostatistic should be an improvement with respect to the geostatistic methods base on classical variogram, because it characterizes the spatial structure by multiple data points, whereas variograms account for correlation between pairs of points only. In other words, MPS replace the variograms by a training image.

A challenge with MPS method is to obtain an adequate training images that correspond to conceptual representations of geologic patterns of the reservoir heterogeneity to be reproduced.

At each grid node, the conditional probability density function (PDF) of the facies is obtained by considering hard data, previously simulated nodes, and training images. In MPS the local conditional simulation is built by scanning the training image using a search mask. The following is the process to create a training image to be used into the facies model in Petrel software:

1. Preconditioning stage

a. Preparing a training grid.

b. Creating training image (TI) in the training grid (TG): in this software training image is a property derived from aerial image, hand drawn images, seismic attribute and it is a simple representation of the geology. A training image or set of training images must be built with the features and same scale as the reservoir model and with sufficient size to provide reliable conditional probabilities for the applied data event template.

2. MPS process

Multipoint simulation uses a sequential simulation. In this method the local conditional distribution is built by scanning the training image. The sequential simulation algorithm determines a path visiting all nodes. A conditional distribution modeled for each node and each value is simulated from the conditional model. The process continues until all N random path of N pixels are visited, then one realization is generated. By seeding another random path then a new realization is done. Only previous simulated values within a specified neighborhood are used for modelling the conditional distribution (Schlumberger, 2011).

The following is a summary of the process:

a. Generating a facies pattern base on a training image. It means scanning the neighborhood relationship between facies in the TI.
b. Specify the search mask to scan the training image. Conditional probabilities are calculated from the training image(s) and stored in a search tree.
c. Running multipoint facies simulation using the facies pattern.

The training image require to have certain characteristics described in the Table 2.

Requirements for training image	
Number of bodies	few geobodies
Number of facies	2 to 6 facies to avoid overtraining
Repeatability	features equally distributed
Fraction	TI and the model should be ideal to have 10% of difference among each facies.

Table 2. Requirements for training image.

In the Figure 1-4 is shown the procedure of multipoint simulation. The search mask is specified for scanning the training image. That process is before to run a local distribution which is calculated by scanning a training image. Location **S** is the current simulated pixel at the simulation grid. Search mask is positioned in the center at **S** location, and four values are within the neighborhood (two are sand (blue) and two are shale (white)); their geometry configuration data distribution is called pattern. This pattern is used to scan the channel image to infer the sand body probability at location **S**.

There are four patterns found in the training image, three of them correspond to sand and one to shale meaning that the probability to be sand at the location **S** is 0.75. Drawing this probability, it gives a simulated value at pixel S, the simulated value is added to conditional data set to constrain the next pixel simulation. The simulation is moved to another pixel location, this sequential process continues until all locations are visited (Schlumberger, 2011).

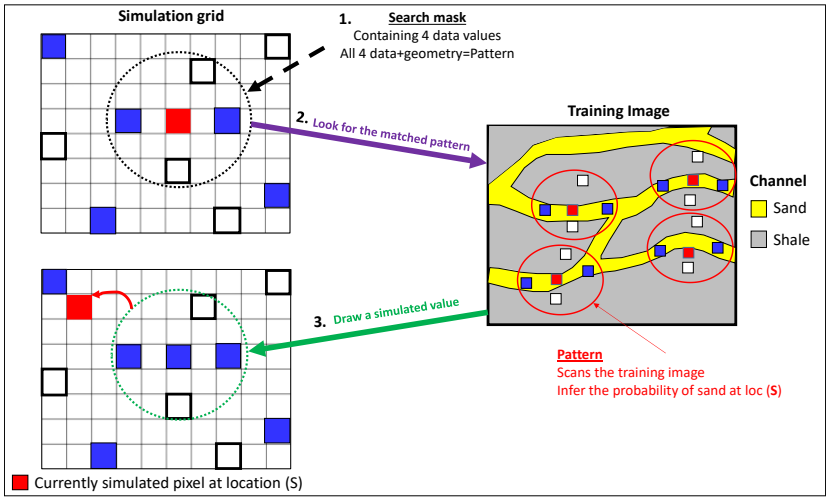

Figure 1-4. Procedure of multiple point simulation (adapted from Schlumberger, 2011).

The spatial correlation in MPS is from one to one at the same time. Training image describes the geological facies in a relative position to each other (Schlumberger, 2011).

1.2.3.2. Property Modelling Methods

Property modelling has the objective to capture the distribution of porosity, permeability, and water saturation in the geocellular model. According to (Cannon Steve, 2018), porosity and permeability should be stochastically modelled. Water saturation should be distributed as height above contact.

The most common methods used in the petroleum industry to model properties are: sequential gaussian and gaussian random function explained in Table 3.

Property Modelling Methods	Characteristics
Sequential Gaussian Simulation (SGS)	• SGS uses kriging as estimator of the mean and variance of the conditional normal distribution from each point. • This method is appropriate to continuous variables. • It is required to transform the input data distribution to have a normal distribution.
Gaussian Random Function Simulation (GRFS)	• GRFS is a faster technique, it is not sequential compares to Sequential gaussian simulation. • This method is based on well-known decomposition of Kriging plus Unconditional Simulation (Jassim M & Mohammed S, 2019).

Table 3. Main characteristics of property models methods.

1.2.3.3. Uncertainty Assessment

Cannon Steve (2018), defines uncertainty as the range which describes equiprobable outcomes or can predict an outcome. To reduce the uncertainty is necessary to take more measurements of a property in order to improve the knowledge of the reservoir.

Uncertainty assessment is generally based on associations between input parameters. This kind of association is handled through Monte Carlo simulation doing several realizations base on the distribution given to the input parameters (Cannon Steve, 2018).

An effort to achieve must be made to identify and account for the various sources of uncertainty. The process of building a 3D reservoir model is originated on several uncertainties parameters; data quality, interpretation and sample representation are particularly crucial at all stages of the workflow.

This method works creating random numbers of uniform distributions between 0 and 1 and it reads the quantile linked with the random number located in the distribution (Pyrcz & Deutsch, 2014). Monte Carlo Sensitivity analysis allows to evaluate the relative impact of each input uncertainty. Through this can be removed the larger uncertainties.

MCS processing consist of a series of calculations varying randomly each measurement and parameter within a given statistical distribution. This distribution named probability density function can be normal, log normal, triangular, uniform etc. The results show a range and distribution of possible answers given the interpretation and the uncertainty of each variable evaluated[2].

[2] Rick, A. (2018). Monte Carlo Processing of Petrophysical Uncertainty. SPWLA.

The law of large numbers is important in Monte Carlo simulation via selecting wide range of unbiased variables from some large number of possibilities, which increase the accuracy of results. Consequently, the more samples taken, the closer results to the mean values driven into a narrow distribution.

In geostatistical modelling, when it is necessary to evaluate the uncertainty, MCS process is applied as it is showed in the Figure 1-5. First, it is necessary to calculate the STOIIP by using facies model and property models (porosity, permeability, net to gross, water saturation etc.), this calculation is called base case. Each model included into the original oil in place represents one realization of each modelling parameter.

This base case is incorporated as an input into the Monte Carlo simulation, these models have uncertainty variables (variograms range (minor, major, vertical), direction, seed etc.) selected by the geomodeler, those variables are going to be iterated according to distribution curves (triangular, uniform, normal, log-normal etc.) associated to each variable. During the MCS' process, random values placed into the selected distribution are estimated. Finally, MCS generates a probability distribution plot through (P10-P50-P90) percentiles.

The result will be different realizations, associated to probability density functions (PDFs). The final product is related to randomly created 'seed' parameter used by the algorithm to generate each realization; (Cannon Steve, 2018).

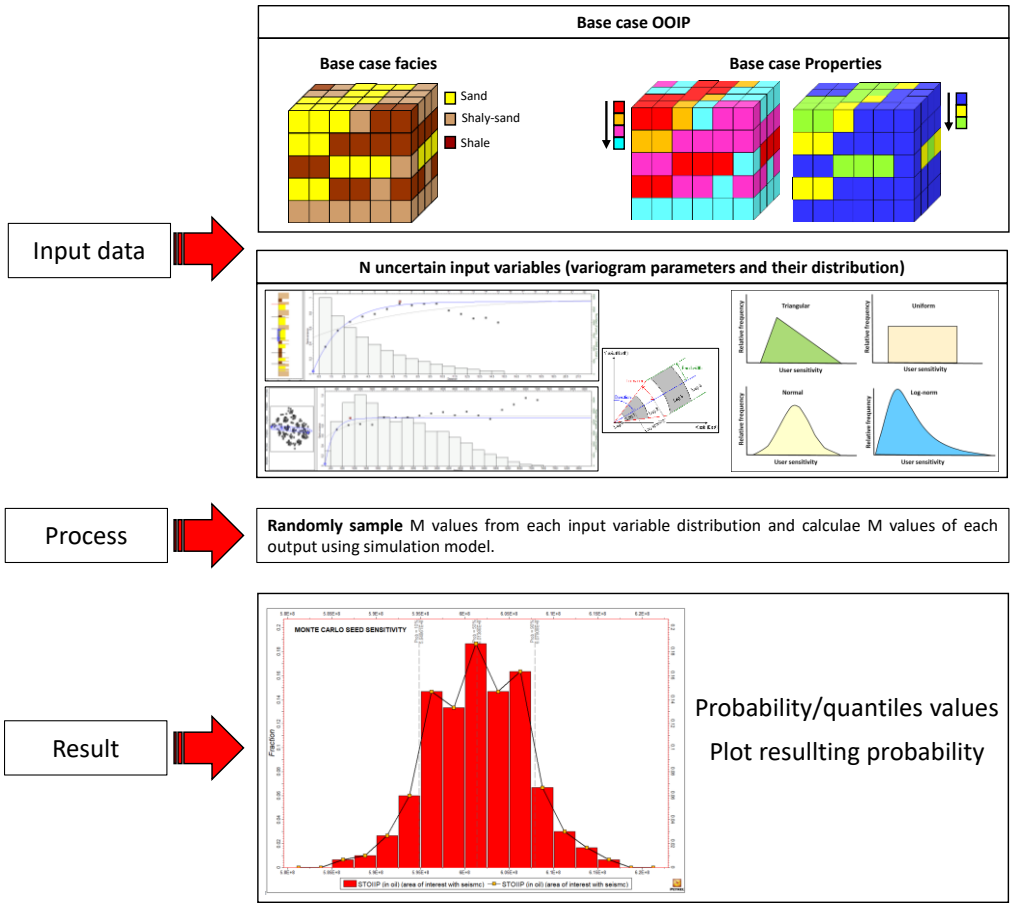

Figure 1-5. Monte Carlo general process 3D static model uncertainty.

1.3. HEAVY OIL

Biodegradation is the main cause of forming heavy oil. Microbial degradation is reached under 80 °C, generating oil oxidation, increment of density, acidity, and viscosity and dropping gas/oil ratio (GOR) (Hussein et al., 2006).

Heavy oil is defined as a liquid petroleum of low specific gravity between 10 to 22 °API. Table 4 shows the oil specific gravity of the oil classes: light, medium, heavy, and extra-heavy.

Oil Class	°API
Light	>=31 °API
Medium	22<= °API <31
Heavy	10<= °API <22
Extra-Heavy	°API<=10

Table 4. Crude oil classification by National Petroleum Agency of Brazil[3].

Heavy oil is commonly associated to giant shallow formations composed of unconsolidated sand. It has low energy, low gas oil ratio (GOR) with high viscosity. It is chemically composed of asphaltenes, resins, saturates and aromatics.

One of the most relevant aspect of heavy oil is its viscosity, because it impacts the recovery and productivity of the reservoir.

1.4. RELATIVE PERMEABILITY

Relative permeability is a measure of the ability of a porous medium to conduct flow of a given fluid in the presence of other immiscible fluid. Relative permeability is defined as the ratio of the effective permeability to a fluid at a given saturation to a reference permeability (for example Kabsolute or Kro@Swi).

According to Archer & Wall (1992), relative permeability definition stablishes the relationship between absolute permeability of the porous media and the effective permeability of a specific fluid in the rock when that fluid only fills a fraction of the total pore volumen.

$$k_r = \frac{k_e}{k_{ref}} \qquad \textbf{Equation 1-2}$$

Where Kr is the relative permeability of the phase, Ke is the effective permeability of the phase (which can be the oil effective permeability -Ko- or water effective permeability -Kw-) and Kref is the reference permeability of the porous rock (Archer & Wall, 1992).

[3] Taken from: Santos, R., Loh, W., Bannwart, A., & Trevisan, O. (2014). An overview of heavy oil properties and its recovery and transportation methods. Brazilian Journal of chemical engineering, 571-590.

The reference permeability can be either the oil relative permeability at Swi (Kro@Swi) or absolute permeability. Laboratory measurement commonly report Kro and Krw using Kro@Swi, then, it is important to recalculate those relative permeabilities using absolute permeability. The absolute permeability is obtained with water or gas, and it is common to use Klinkenberg Permeability, which is the gas permeability corrected at reservoir conditions as the absolute permeability. In this study, all the relative permeabilities use Klinkenberg permeability as reference permeability.

Oil and water are present in the reservoir, these fluids interfere and the effective permeability to oil flow (ko) will decrease while water flow (Kw) increase during production stage (Figure 1-6).

One observation is that the sum Krw and Kro are less than absolute permeability. This fact shows that the permeability is affected when 2 or more fluids coexist in the porous media.

1.4.1. Laboratory Water Oil Relative Permeability

Figure 1-6a represents relative permeabilities of two phases system: water and oil in this case, which are expressed as a function of water saturation (Sw). The maximum water saturation occurs when the oil phase (curve green) reaches the residual oil saturation (Sor), this illustrates the immobile oil zone (right side of the image), sometimes this is not only observed as microscopic level but also at macroscopic level covering big geographic areas known as residual oil zones (ROZ). That means water is displacing oil until the oil is not able to move.

Figure 1-6b shows the summary of the relative permeability test in lab under unsteady state condition. The process begins with a plug 100 % saturated by water which means the permeability in that condition is absolute. Next, oil is injected to constant rate until it reaches irreducible water saturation (Swirr), at this point the oil relative permeability at Swi is obtained (kro@Swi).

The final step is injecting water and the oil and water relative permeabilities points for both phases are calculated once the breakthrough happens. Water is continuously injected until it reaches the residual oil saturation where no more oil is able to be displaced and water relative permeability at residual oil saturation (kro@Sor) is calculated. During the test the injection rate is constant and water and oil production is monitored, together with a constant pressure differential.

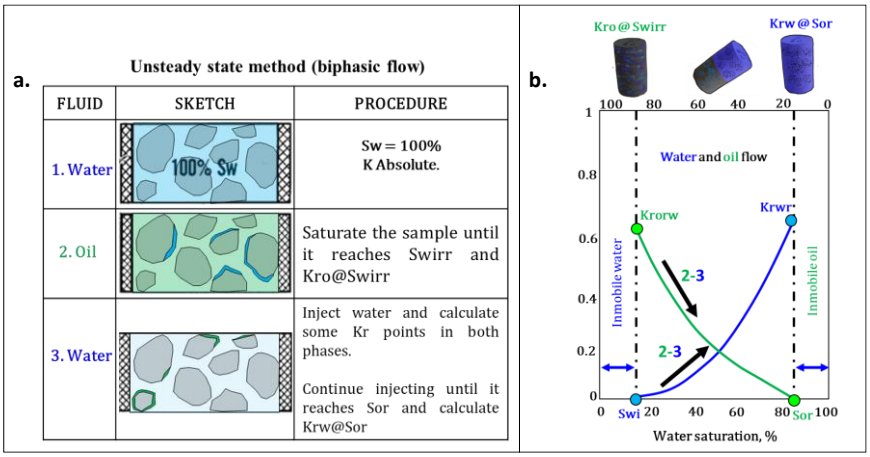

Figure 1-6. a. Representation of relative permeability curves. b. Simple sketch of relative permeability lab procedure.

1.4.2. Corey Correlation Water - Oil System

Corey correlation is the most common correlation used to correlate the relative permeability points obtained in the laboratory.

This model assumes the wetting and non-wetting phase-relative permeabilities to be independent of the saturations of the other phases and requires only a single suite of water / oil-relative permeability data.

To used Corey Correlation, it is assumed that relative permeability is at constant pressure, temperature, viscosity, Interfacial tension, composition

The equation 1-3 and 1-4 are the Corey oil and water correlation respectively. This correlation uses the endpoints and the parameter n_o and n_w (related to shape) to fit measured points.

$$k_{ro,\,min/Max} = k_{ro}@S_{wirr} * \left(\frac{1-S_w-S_{or}}{1-S_{wirr}-S_{or}}\right)^{n_o} \qquad \textbf{Equation 1-3}$$

$$k_{rw,\,min/Max} = k_{rw}@S_{or} * \left(\frac{S_w-S_{wirr}}{1-S_{wirr}-S_{or}}\right)^{n_w} \qquad \textbf{Equation 1-4}$$

Where:

k_{ro} : Relative oil permeability.
k_{rw} : Relative water permeability.
n_o : Corey & Brooks oil exponent.
n_w : Corey & Brooks water exponent.
S_{or} : Residual oil saturation.
S_{irr} : Irreducible water saturation.
S_w : Water saturation from 3D model.

1.4.3. Heavy Oil Relative Permeability.

Heavy oil Relative Permeability has a special condition as it depends not only on water saturation but also on viscosity, rate, and pressure as show by Torabi Farshid.

Cao et al. (2014) and Torabi Farshid (2016) showed the effect of temperature on the relative permeability. Water and oil are significantly temperature dependent and increase when the temperature rises.

Mai An (2008) showed that capillary number is not the best adimensional number to correlate the dependency of relative permeabilities, instead the instability number has shown some correlation with oil recovery factor. Instability number is also frequently used to identify if relative permeabilities are reliable or not[4].

[4] J.S Archer Petroleum Engineering Principles and Practice Book. Page 110

$$I = v \cdot \mu \cdot D \qquad \textbf{Equation 1-5}$$

Where I is instability number, v is the injected velocity (m/s) μ is viscosity of the fluid (mPa×s) m is D is diameter of the sand pack (m).

When the instability number is less than 1 the data collected is not representative of true relative permeability. In other hand when it is larger than 1 the breakthrough does not change by changing viscosity or injection rate; the point of stabilized flow is where the capillary effect ends. (Mai, 2008).

1.5. PRESSURE BUILD UP

A pressure transient test is used to measure the pressure changes in the reservoir in production or injection mode. The pressure build up is one of many others pressure transient analysis (PTA) techniques. The Pressure Build-up (PBU) is a test where a well is producing at stable conditions (constant rate) while the pressure is being recorded as close to the perforated interval as possible. Then, the well is shut in the pressure that was originally declining due to production suddenly begins to build up trying to reach the reservoir pressure.

The pressure build up is the Bottom hole pressure (BHP or Pwf) that is recorded in the well. By using an analytical model, it is possible to link the rate before the shut in and the bottom hole pressure that is building up to obtain several characteristics of the porous media like flow capacity (Kh) and skin.

Figure 1-7 is a graph of a theoretical example of PBU test. The red dots correspond to pressure measurement taken in a specific point in the tube, the rates change is related to changing choke sizes which generate disturbance into the reservoir (high choke size= high rate = less pressure). The well is closed in a determined period of time, in this case at 100 hours (pressure build up test). This graph shows a PBU test designed in W-091 belonging to the AOI.

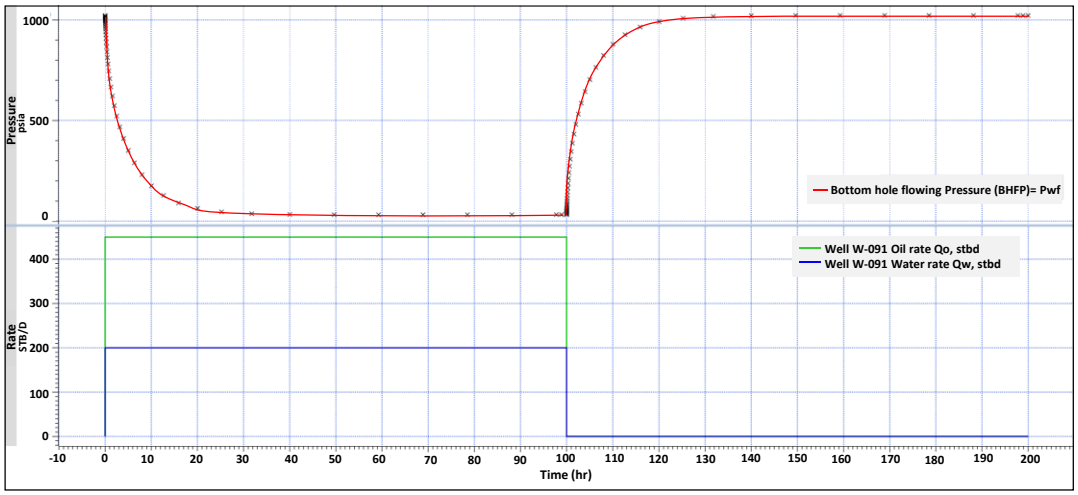

Figure 1-7. PBU test in W-091 that belongs to AOI.

For this study, the pressure derivative is quite complex as it is affected by a constant pressure support coming from an active aquifer and high oil viscosity (Figure 1-8). These characteristics masks a clear infinite acting radial flow (IARF) which is highlighted in black in the figure below, the late time region

(LTR) shows the derivative going down because of constant pressure support boundary does not allow the Pwf to change anymore at late time.

Derivate method has the pressure derivative and the pressure difference in Y axes versus time in the X axes. This method is commonly used in heterogenous reservoirs and differents flow regimes, in other words this method is applied to complex reservoirs (Figure 1-9).

These pressure perturbations are evaluated using mathematical/analytical models to estimate: effective permeability, skin, reservoir pressure, boundaries (aquifer support, faults, etc.)

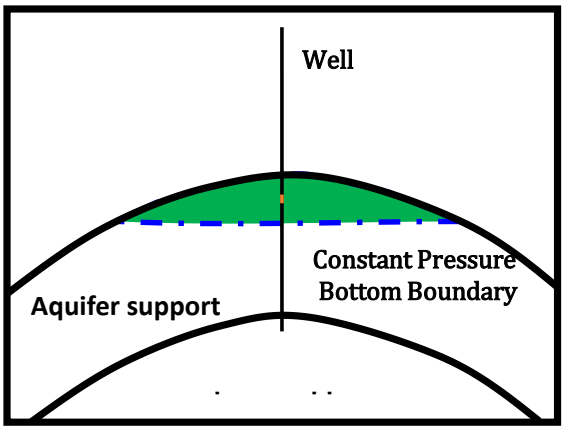

Figure 1-8. PBU conceptual model.

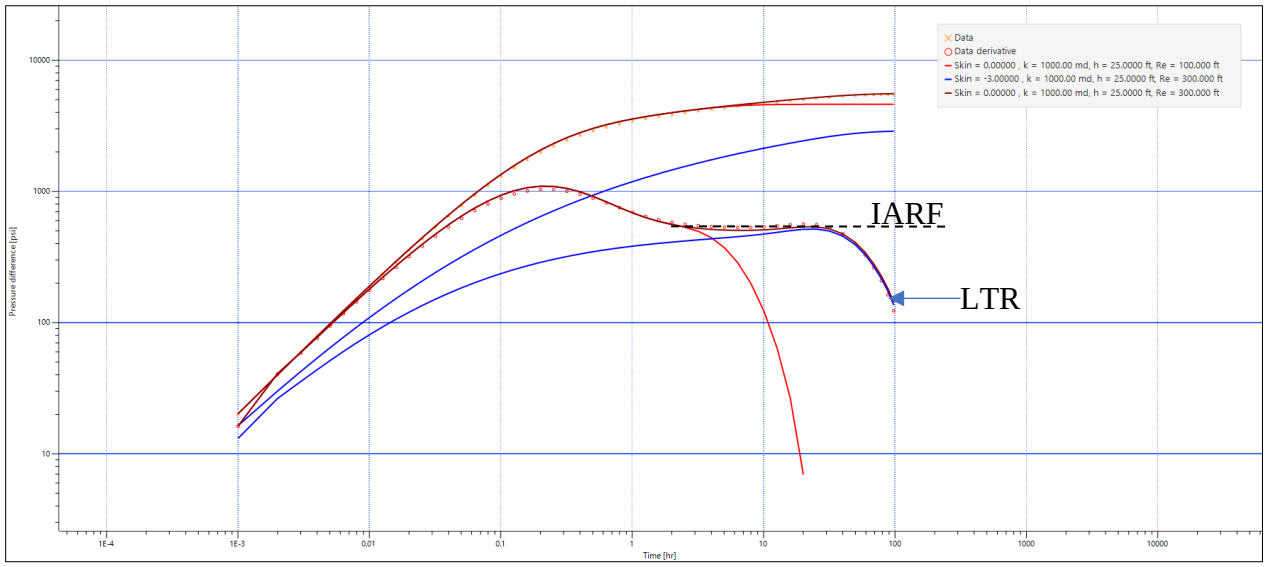

Figure 1-9. Ideal behavior of pressure derivative.[5]

[5] Notice how an interpreter can easily miss to select the right IARF, this might underestimate the KH of a well.

1.6. OIL RATE CALCULATION

The initial oil rate represents the measurement how many barrels of oil per day a new oil well produces. It is used as an approximation for an oil wells future productivity.

In this project instead of focusing on building complex dynamic models, it is proposed as the first step to estimate the possible initial rate that a hypothetical vertical well might have if drilled in every grid cell, this step is never used by a geomodeler while building a static model. Vertical wells are the most convenient wells as they can be used to calibrate the expected productivity of alternative drilling geometries and completions such as horizontal wells.

Reservoir simulation uses complex equations to link the well with the reservoir, but for practical purposes the solution of the diffusivity equation for steady state and radial flow conditions can be used to perform a very good quality control to the static model. Rate calculations should give reasonable results compared with historical data to validate or discard some geological realizations.

If it is observed that wells are underperforming it means that there is some parameter that needs to be reviewed. It is very common to use transmissibility multipliers in reservoir simulation to achieve a history match of pressure and production data. By doing the step of checking the expected initial rate in the static phase modelling section, it helps to avoid future distortions and modification in the dynamic modelling phase.

As described by several authors[6], steady state solution for radial flow conditions for ideal liquids using field units can be described as follows:

$$Q_o = 0.00708 \frac{K_{ro} * K * h}{\mu_o \cdot B_o} * \frac{(P_{res} - P_{wf})}{ln\left(\frac{re}{r_w}\right) + s - 0.75} \qquad \textbf{Equation 1-6}$$

Steady state flow happens when the reservoir pressure is constant with time, which is this case due to the constant pressure support provided by the aquifer.

Where :

Qo : Oil rate, stbd.
K : Klinkenberg permeability, md.
Kro : Oil Relative Permeability, adimensional.
Pres : Reservoir Pressure, psia.
Pwf : Bottom hole flowing pressure, psia.
re : External radius, ft.
rw : Well radius, ft.
s : Formation damage, also known as skin, adimensional.
h : Net Thickness, ft.
Bo : Oil volumetric factor, rbbl/stb.
μ_o : Oil viscosity, centipoise (cp).

[6] This study used Michel Golan and Curtis H. Whitson. Well Performance. Second Edition. 1996 Chapter 2 as reference to describe Initial Oil Section.

1.7. PRODUCTIVITY INDEX

The productivity index is obtained by simultaneous measurements of surface production rate and bottomhole pressure (Golan & Whitson, 1991). In other words, productivity index defines the ability of a well to produce hydrocarbon.

The inflow performance relation (IPR) is used to define the relationship between surface rate (q) and flowing bottomhole pressure (Pwf). The most common used IPR equation is the straight line IPR which states that rate is directly proportional to pressure drawdown in the reservoir. The constant of proportionality is called productivity index (Jo) which is defined as a ratio of oil rate to a drop pressure difference between the reservoir pressure and the bottom hole flowing pressure (Golan & Whitson, 1991). PI is written with the following equation:

$$J_o = PI_o = \frac{q_o}{(P_{res} - P_{wf})} \qquad \textbf{Equation 1-7}$$

Where:

J_o : Productivity index, stbd/psia
q_o : Oil rate, stbd

The following equation works under saturated oil, meaning that Pwf will be above the bubble pressure[7].

$$Q_o = J_o\left(P_{res} - P_{wf}\right) \qquad \textbf{Equation 1-8}$$

Production Index named as PI or J has stb/psi units is defined in Equation 1-9. Notice that this equation does not have reservoir or bottom hole flowing pressure. Meaning of that it can be used with the static model.

$$J_o = PI_o = \frac{K_{ro} \cdot K \cdot h}{141.2 \cdot \mu_o \cdot B_o \cdot \left[ln\left(\frac{r_e}{r_w}\right) + s - 0.75\right]} \qquad \textbf{Equation 1-9}$$

Where:

PI = Productivity Index, stb/psia.

When it is necessary to infer Pwf in cases where PTA are not available, the bottomhole pressure can be calculated through the Equation 1-10.

$$P_{wf} = \frac{Q_o}{J_o} - P_{res} \qquad \textbf{Equation 1-10}$$

[7] Bubble Pressure: defined as the pressure at which the first bubble of gas appears at a specific temperature.

2. AREA OF INTEREST: MAIN CHARACTERISTICS

This section shows the most relevant features belonging to the area of study such as location, local and regional geology, well petrophysical model, and reservoir engineering aspects.

2.1. STUDY AREA LOCATION

The AOI spans 8700.19 acres and is located in the Meta department, in the southeast area of the Llanos Basin. This area is limited by Villavicencio and Andes Mountain ranges to the east, Guaviare department to the south, Vichada department to the east and Sabanero field to the north. (Figure 2-1).

The sector selected exhibits special structural, stratigraphy and oil migration characteristics compared to the rest of the basin.

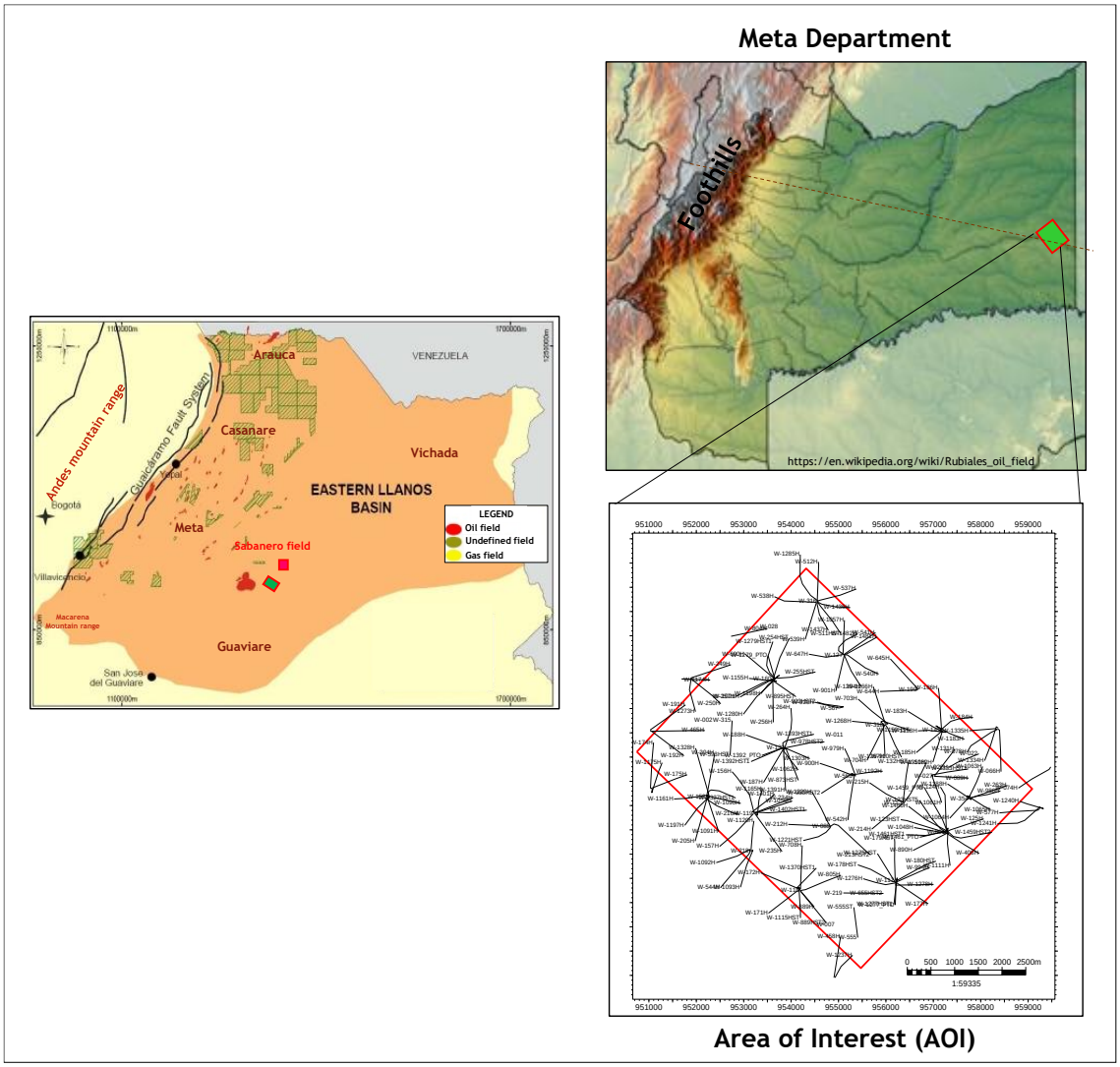

Figure 2-1. Area of interest location.

2.2. REGIONAL GEOLOGY

Eastern Llanos Basin is defined as foreland basin. This basin has an active margin to the west and a passive or stable margin to the east. This characteristic helps to understand the stratigraphy and sedimentation process. The general basin structure belongs to a monoclinal with different subsidence periods from Paleozoic to late Tertiary.

The basin rises progressively in the West - Southeast direction, being affected by normal and inverse faults with random slip.

Cretaceous and Cenozoic rocks are lying discontinuously over pre-cretaceous units and their distribution depends on the paleo-topography of the oldest rocks. Some pinch outs are Southwest-Northeast, (Figure 2-2). During Paleocene to middle Eocene happened an erosion period in Llanos basin and emerged Central Range. The eroded material was transported towards the center of the basin in the current Eastern Range and goes also to the north depositing Barco, Los Cuervos and Mirador formations in Foothills.

On the other hand, the Cenozoic sediments far in the east starts with the Carbonera Formation deposited during the Oligocene which distributed sediments in the Western area also. The source of these sediments where the craton and the largest thickness are found is in the west close to Piedemonte (Figure 2-2).

Carbonera formation deposited during the Oligocene starts with the sediments of the operational units called Carbonera C8 and C7, the last deposits covered the wider portion of the basin. Unit C7 is the most important reservoir in this area of study and its thickness increase to the west and decrease to the east (Figure 2-2).

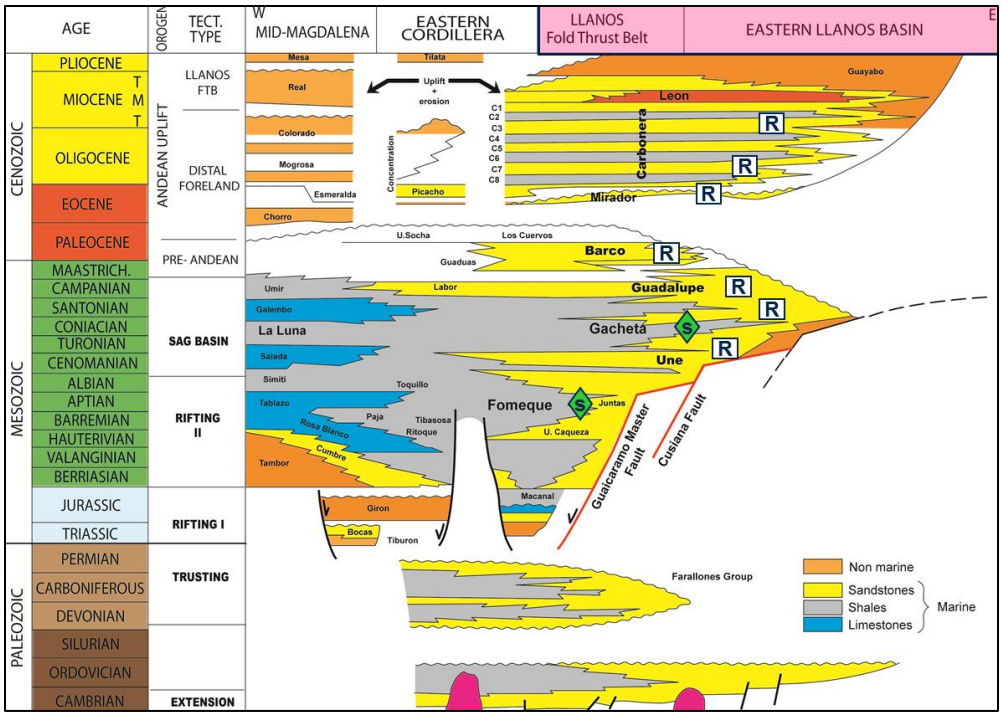

Figure 2-2. Regional stratigraphy chart (adapted from Alfaro, C & Alvarado, I. 2014).

2.3. LOCAL GEOLOGY

2.3.1. Local Stratigraphy

Locally this sector has a sedimentary sequence from Paleozoic to quaternary deposits. This sequence lay on the igneous basement. The basal part of the Cenozoic (Carbonera C8, and the whole Mesozoic sediments are absent in this sector of the basin.

The sedimentary succession deposited in this area correspond to Quaternary deposits, Guayabo, León, Carbonera Formation and Paleozoic (Figure 2-3).

Here it will be described Paleozoic and Carbonera C7, the other units and formation were not incorporate into the geostatistical model. Although Paleozoic was not incorporate in the model but it is important as the lower contact of C7 and it controls the deposition of the upper units in the AOI.

Paleozoic

The bottom part of Paleozoic is composed of carbonates, shales, conglomerates and quarzites. These lithologies are found in the west part of the llano's basin. The upper part of the lower sequence covers almost 70 percent of the basin and it is composed of gray and black fossil shales intercalated with sandstones, this lithology is correlated with Farallones group.

Paleozoic sediments are unconformable lower limit between Cambrian- Ordovician sediments with crystalline basement.

Paleozoic sediments have been contacted in the area of study through vertical wells which drilled a few feet and their description correspond to very thigh sandstones. The clearest recognition of these sediments is based on electrical o seismic signal.

Carbonera

Carbonera Formation in this sector of the basin has seven units from Carbonera C1 to Carbonera C7 (Figure 2-3). The Last member of Carbonera is informally called Arenas Basales (regionally known as Carbonera C7). This formation does not have outcrops, then the description belongs to well cuttings, cores and well logs behavior.

Carbonera C7 represents the bottom of Carbonera Formation and it is the reservoir in this area. It has a thickness variation from 130 to 240 feet. This unit is composed of quartz sands with some variation in grain size intercalated with shales or claystone. In general, those sandstones are well sorted with some coal layers.

In this field, this reservoir unit is divided in nine zones, (Figure 2-3). The first four zones are the most important producers and the last four have likely the oil water contact, that is why some of them are not commercial.

The bottom contact is unconformable with Paleozoic and the top is gradational with the shales of Carbonera C6.

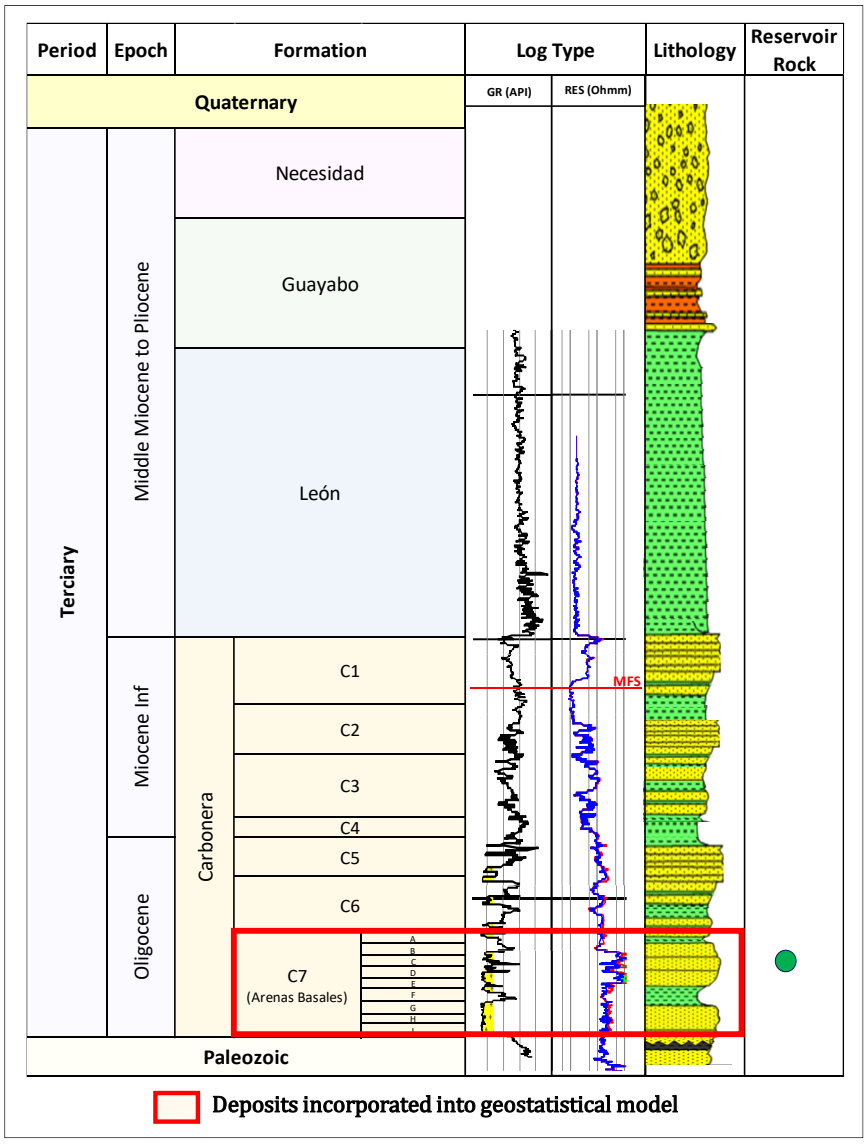

Figure 2-3. Local stratigraphic column.

2.3.2. Local Structural Geology

The AOI belongs to a homocline which dip slightly one degree to Northwest. It has high degree normal faults with small vertical slip and they cut the basement and tertiary formations (including reservoir rocks). Specifically, in this area, those faults do not represent any compartmentalization or impact on the production due to their small slip (under 5 feet). Also, the structural component does not have any strong effect over oil accumulation (Ecopetrol, 2017).

Seismically the faults are interpreted but in the 3D modelling, they are not included, because they do not play an important effect on the accumulation which helps to avoid including unnecessary complexities in simple model. Structure is deepening to Northwest with slight dip as shown in Figure 2-4.

The 3D seismic volume was reprocessed to clean the acquisition footprints, pull ups, statics, and residuals. The new seismic interpretation is in process that it is why the structural features were only mentioned in this study.

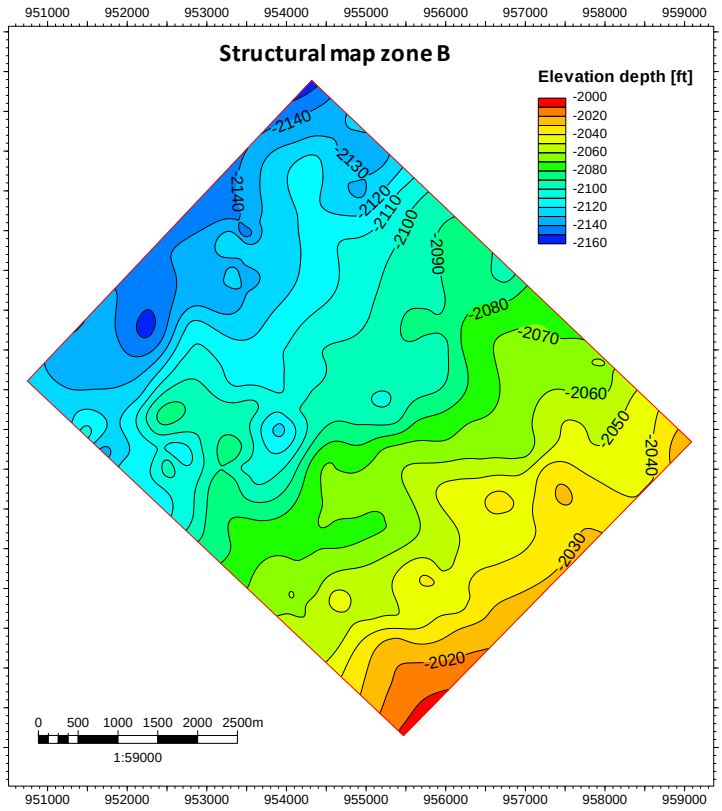

Figure 2-4. Structural surface from well tops to Carbonera C7 zone B.

2.4. SEDIMENTOLOGICAL MODEL

The information described here is taken from Ecopetrol S.A. reports.

The wells logs and cores were the most powerful information to interpret the electrofacies and their depositional environment. This model was built by Ecopetrol S.A.

In this area, the sedimentologic distribution is the most important variable which controls the oil accumulation and the aquifer as it has a significant impact in the static and dynamic model. The sediments accumulation depends on the Paleozoic geometry, nevertheless in the area selected in this study, it does not affect significantly because the Paleozoic geometry does not have important changes in its structure (Figure 2-5).

Lateral facies change has shown the importance to have successful drilling campaigns as it highly impacts the well production results. It was identified that the facies model was key to understand the bodies distribution to properly locate the vertical and horizontal wells.

The methodology applied to build the sedimentological model starts with well logs and cores. Those resources help to identify the well tops, electrofacies, depositional environment (core description) (Navas, 2016).

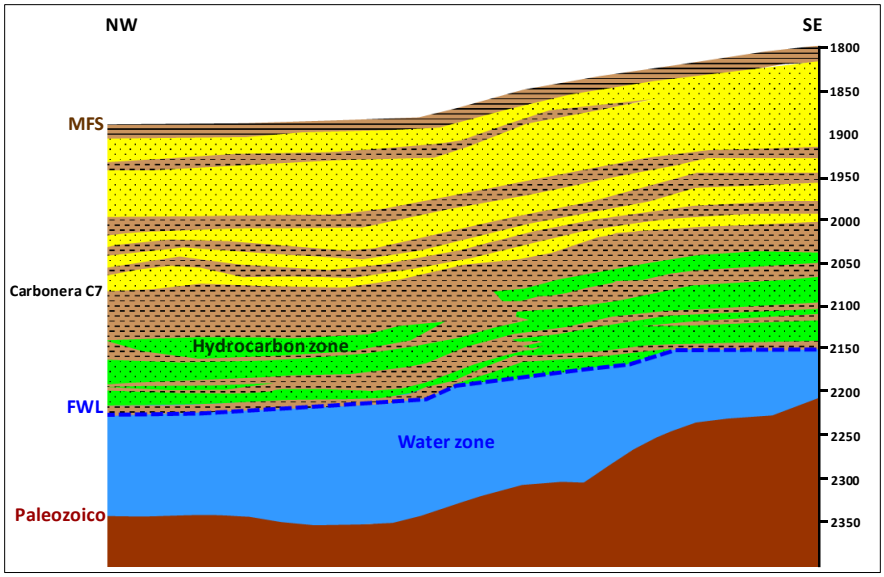

Figure 2-5. Squematic cross section of area of interest. [8]

2.4.1. Well Tops Interpretation

In 2014 it was built the sedimentological model; picks were interpreted with geological and stratigraphic sense. All wells were tie to a regional MFS located in the first Carbonera units precisely between C1 and C2.

The sedimentologist divided Carbonera C7 in nine zones (see Figure 2-3). The internal division was done using electrical rock behavior, thickness, and core data. In the area of interest, the oil accumulation is associated to upper zones of Carbonera C7 (zone A, zone B, Zone C, and zone D) (see Figure 2-5).

Base on the well logs it is defined each stratigraphic zone has a depositacional sands extension with potential to accumulate hydrocarbons, those zones change their facies laterally and his grain size changes as well, so this condition reduce their potential, even more in this case when their fluid is heavy oil.

2.4.2. Core Analysis

There are only two cored wells in this AOI, W-130 with poor sample recovery and W-158 with good sampling (Figure 2-6). The AOI belongs to this full field sedimentological model which has much more cored wells.

[8]FWL: Free water level.
MFS: Maximum flooding Surface forms during the culmination of relative sea-level rise, and the maximum landward translation (flooding) of the shoreline.

Core data helped to identify and confirm lateral facies changes, environmental patterns which control facies deposition, seal rock types identified in the logs. It was defined the condition of lateral facies variations which are controlling the oil accumulation in the reservoir using this information.

The core analysis defined that Carbonera C7 is composed by sandstones with grain size variation from conglomeratic to very fine sand, mainly composed of quartz and some samples that has feldspars such as secondary mineral. These sandstones are very fragile and it is easy to guess high porosities which is corroborated by stain evidence in the core. When this data is tie with production, it confirms the good properties of this sand (Navas, 2016).

The basic core analysis reports porosities between 25% and 35% with permeabilities between 100 and 20000 milidarcies.

The main facies identified in Carbonera C7 belong to fluvial deposits. Nevertheless, some sections in W-158 have facies of tidal influence (Navas, 2016).

- **Laminated Sandstone Facies:** It is a Subarkose, very fine grain size, well sorted, wavy laminated and with ripples. Locally has organic material. This facies does not have stain.

- **Sandy with Bioturbation Root Facies (Fsnbr):** This facies presents normal gradation and it is composed of very fine to medium grain size sandstones (quartz sands with felspar). It has a poor sorting with plants prints. Locally it is slightly stained. In some cases, it has siltstones completely bioturbated (Figure 2-6).

- **Sandy Facies (Sn):** It is a coarse-grained size sands with normal gradation, subarkoses with some quartz in the top. They have poor and moderate sorting with subangular and sub rounded particles and they are highly stained by hydrocarbons. In the Figure 2-6 at 2769 feet this facies can be found.

- **Bioturbated sands Facies (Snb):** It is a medium to fine grain size subarkoses, normal gradation, poor sorting with sub-angular and subrounded. This facies is highly bioturbated with relict of laminations and cross lamination.

- **Bioturbated Shales Facies (Fsb):** This facies has Siltstones completely bioturbated in some case present cylinder borrows filled by sand. (Figure 2-6).

- **Laminated Shales Facies (Fcl):** This facies is a dark gray siltstones with planar parallel lamination. (Figure 2-6)

- **Intercalated Sandstones with Shales Facies (IFS1):** Very fine sands, well sorted with planar wavy lamination with intercalation of dark gray siltstones. In the Figure 2-6 at 2749 feet this facies is found.

- **Intercalated Sandstones with Shales Facies (IFS2):** Sandstones with some levels of claystone. Coarse grain subarkoses, poor sorting with angular and subangular grains. Beige kaolinitic claystone.

- **Intercalated Sandstones with Shales Facies (IFS3):** Dark gray siltstones with planar parallel lamination to slightly wavy, presents fine, well sorted sandstones with wavy lamination and ripples.

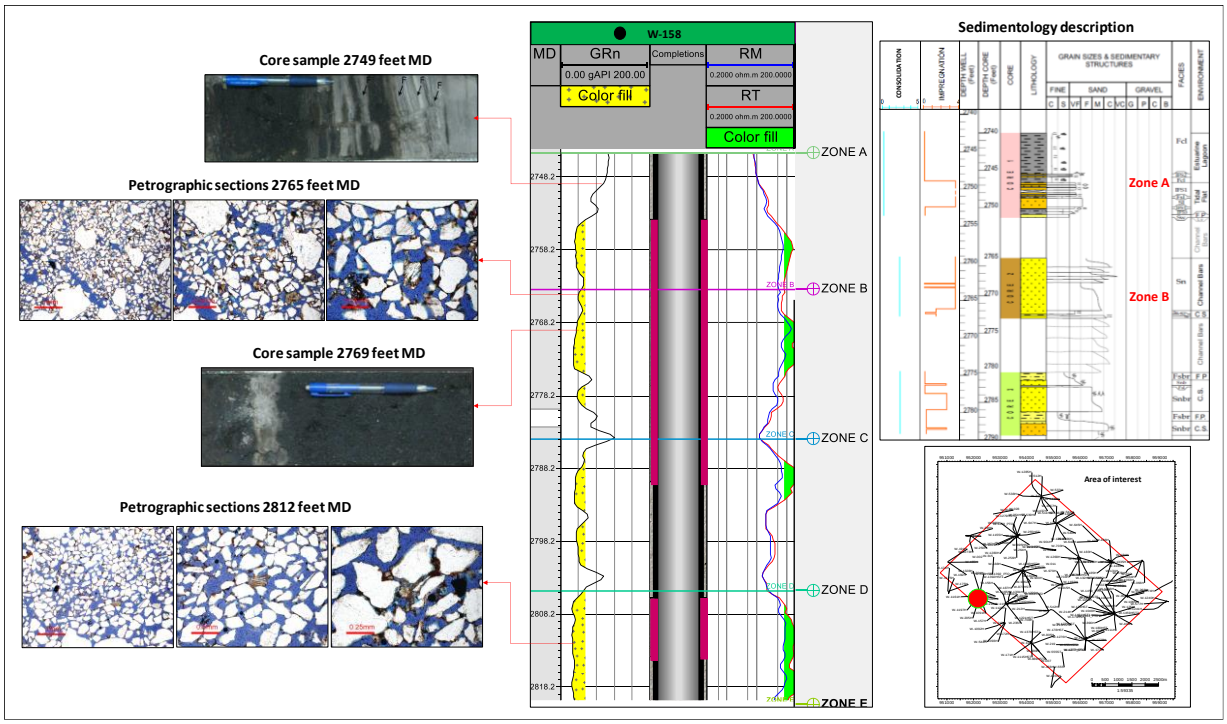

Figure 2-6. Core and samples in the zone of interest and sedimentological description well W-158 (adapted from Ramirez, 2010).

2.4.3. Depositional Environment Association

Presence of root footprints indicate a reduction of flow regimen and therefore a lot of plants invade bottom deposits. Facies association Sn and Snbr are interpreted as gradually abandoned channel "chute cut of"[9]. Silt and shale accumulate by suspension in subaqueous spaces. Bioturbated siltstones and shales with organic material (Fsb) represent swamps and facies Fsbr belongs to floodplain deposits. The zones more suitable to develop coal are river and salt marsh back marsh[10]. Therefore, facies association Fcl belongs to marsh deposits (Figure 2-7).

In general, Carbonera C7 cores were interpreted as fluvial environment (bed load, and mixed load) for example in W-158 well core was identified some facies of barrier channel and this electro-shape is associated to facies with high hydrocarbon accumulation. Nevertheless, some cores sections show a transition deposit which is a complex depositional system with lateral facies changes. Those facies must be characterized due to they control hydrocarbons accumulation and potential sand bodies distributions, (Navas, 2016).

[9]Cant, D. J., & Walker, R. G. (1978). Fluvial Process and Facies Sequences in the Sandy Braided South Saskatchewan River. Sedimentology, 25. Retrieved from https://doi.org/10.1111/j.1365-3091.1978.tb00323.x

[10] Takano, O., & Waseda, A. (2003, August). Sequence Stratigraphic Architecture of a Differentially Subsiding Bay to Fluvial Basin: The Eocene Ishikari Group, Ishikari Coal Field, Hokkaido, Japan. 160, 138-156.

The tops between zones are flooding surfaces, erosional surfaces, and paleo-soils which divide the reservoir in nine zones and they in some cases can create compartmentalization where the seals have low permeability with wide areal extension. Also, those zones can generate vertical water flow barriers and different production and pressure drops behavior by zone, (Navas, 2016).

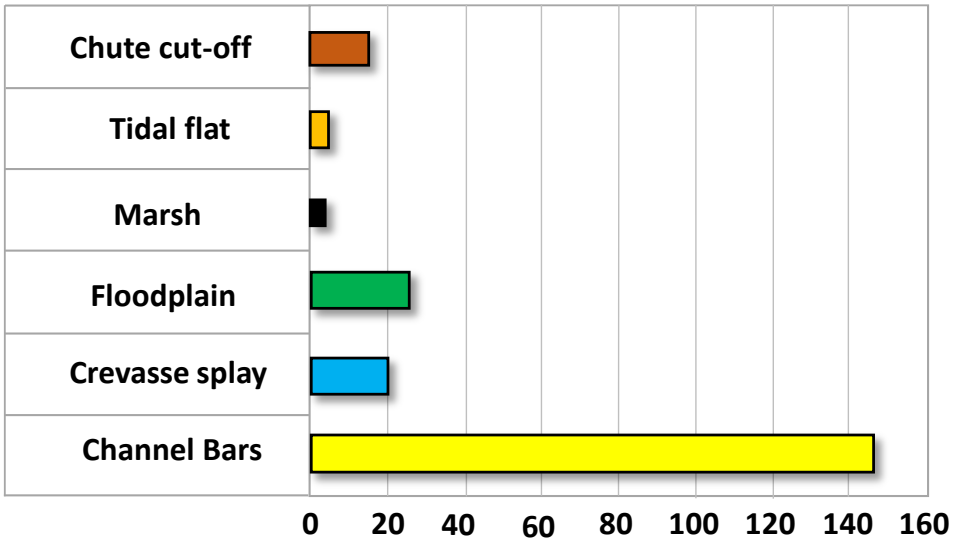

Figure 2-7. Thickness of the environments interpreted in Carbonera C7 found in W-158.

2.4.4. Facies Distribution Maps by Zones

Facies maps integrates well logs data and core description. Those maps were built with the electrical shape of lithological log generally Gamma ray (GR), this log behavior is called log signature (electrofacies) and it reflects grain size changes and mud content allowing the assignment to a specific depositional environment (Figure 1-1).

There were identified four factors which control the rock stain (Ecopetrol, 2017):

- **Bioturbation:** this activity reduces the porosity due to roots, debris, and burrows. This reduction generates more tortuosity and decrease the flow capacity. The stain here is not homogeneous is scarce by patches.
- **Grain size:** very fine material belongs to small pore throat radius even in well sorted rocks, due to the low flow capacity of the heavy oil.
- **Lithology (facies):** siltstones and shales do not have stain, as well as some sand with shale matrix.
- **Potassium content:** the increment of potassium content lessens the stain even producer sandstones.

Base on core analysis and logs interpretation the sediments of Carbonera C7 were deposited in high energy fluvial environment, but some zones have evidences of tidal influence which comes from west to east and the transition are identified in the upper part of Carbonera (Navas, 2016).

2.4.4.1. Zone A

The best oil production of this zone belongs to cylindrical GR shapes, fining upward electro facies has a restricted oil accumulation, it has a small net pay thickness and finally coarsening up and serrated electrofacies do not have prospectivity in this zone (Navas, 2016).

Figure 2-9a shows the facies distribution along of the area of interest. Green color belongs to serrated electrofacies, blue coarsening up, yellow fining upward and orange block or cylindrical.

The channels are towards west, the predominant prospective facies is fining upward (yellow color in the Figure 2-9a) followed by cylindrical. Nevertheless, serrated is the dominant facies in this area (green color in the map Figure 2-9a). This facies does not have the capacity to accumulate oil as its grain size is very fine.

Wells which drain to this zone they do it from fining upward and cylindric electrofacies. Both have the highest oil production wells in this zone. Those facies are in the center south of AOI.

In this zone of the AOI the depositional energy has decreased, this zone is interpreted as a transitional environment with tidal flat lagoon. Evidence of this is the sedimentary structures and fossil association. It was found a wavy laminated shales, very fine grain size and well sorted rocks indicating channels with tidal influence (Figure 2-6).

Fluvial sediments were moving to west, producer wells in zone A are located in this direction and the river mouth was distributed in high number of channels, which could be evidence of deltas formation with fluvial domain.

According to Figure 2-6, this zone has the following facies Fcl, IFS1, IFS2 and IFS3, they are associated to estuarine lagoon and tidal flat environment.

2.4.4.2. Zone B

Zone B facies are associated to fluvial deposits where cylindric facies have excellent petrophysical properties, they are interpreted as channel bars and defined as high oil accumulation zones (Figure 2-6). The horizontal wells which drain this zone has the best initial production in this area over others facies and zones. (example W-512H, W-250H and W-593HST had an initial oil rate production over 500 bls)

The preferential sediments deposition was east to west, in that direction are interpreted fining upward, coarsening upward and cylindric facies (yellow, blue, and orange respectively according to Figure 2-9b). The first facies have more restricted properties to accumulate oil. Now some rocks can have good properties but they can also have their free water level very close, so that relative position to the FWL affects oil accumulation due to the low oil mobility compared to the water.

In general, all facies are at the same proportion in the area except to fining upward facies, it has a slightly less proportion than the others (Navas, 2016). The south part of the area of study has less prospectivity in this facies, because there it is mainly a serrated facies (Figure 2-9b).

2.4.4.3. Zone C

This zone has facies associated to high deposition energy. The most common electrofacies is fining upward followed by cylindric and coarsening upward (Figure 2-10a). The highest deposition energy sediments were in the south west part of AOI represented by cylindric facies (orange color in the Figure 2-10a).
In general, some wells which are opened in zone C are also opened in zone B and their initial oil rate is random.

Zone C has potential in facies cylindric, fining and coarsening upward, however the last facies have less oil productivity than the first one (cylindric). Rocks associated to zone C were deposited in a fluvial environment, meander, crevasse splay and channel bars deposits (Navas, 2016).

2.4.4.4. Zone D

Deeper facies are related to high deposit energy as seen in the previous zone facies and the actual zone. Serrated facies are disappearing completely (Figure 2-10).

Zone D sediments were deposited in direction East-West, their depositional environment is fluvial, according to the sandy section cored in W-158 well. In this zone those deposits belong to channel bars (Figure 2-8).

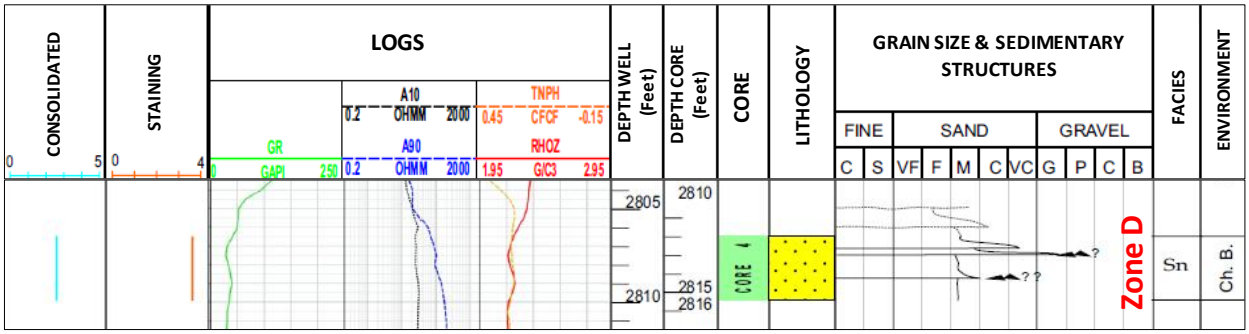

Figure 2-8. Sedimentological description of zone D well W-158.

In the central region of the AOI, the predominant facies are cylindric and fining upward and those facies have capacity to storage oil like coarsening upward found in the north and south part (Figure 2-10b). The coarsening facies are discontinuous between fining upward and cylindric facies.

The deeper zone is the closest one to the water zone (FWL) that means they can have high water cuts and the bottom part of this zone in general does not have oil are filled with water.

The most of completions in vertical and horizontal wells are in the upper part of Carbonera C7 up to zone D. Nowadays with a new analysis (seals, sands distribution and pressure data analysis) developed by Ecopetrol they have opened deeper zones with excellent results because they are identifying the extension of the seals and the vertical connectivity (Navas, 2016).

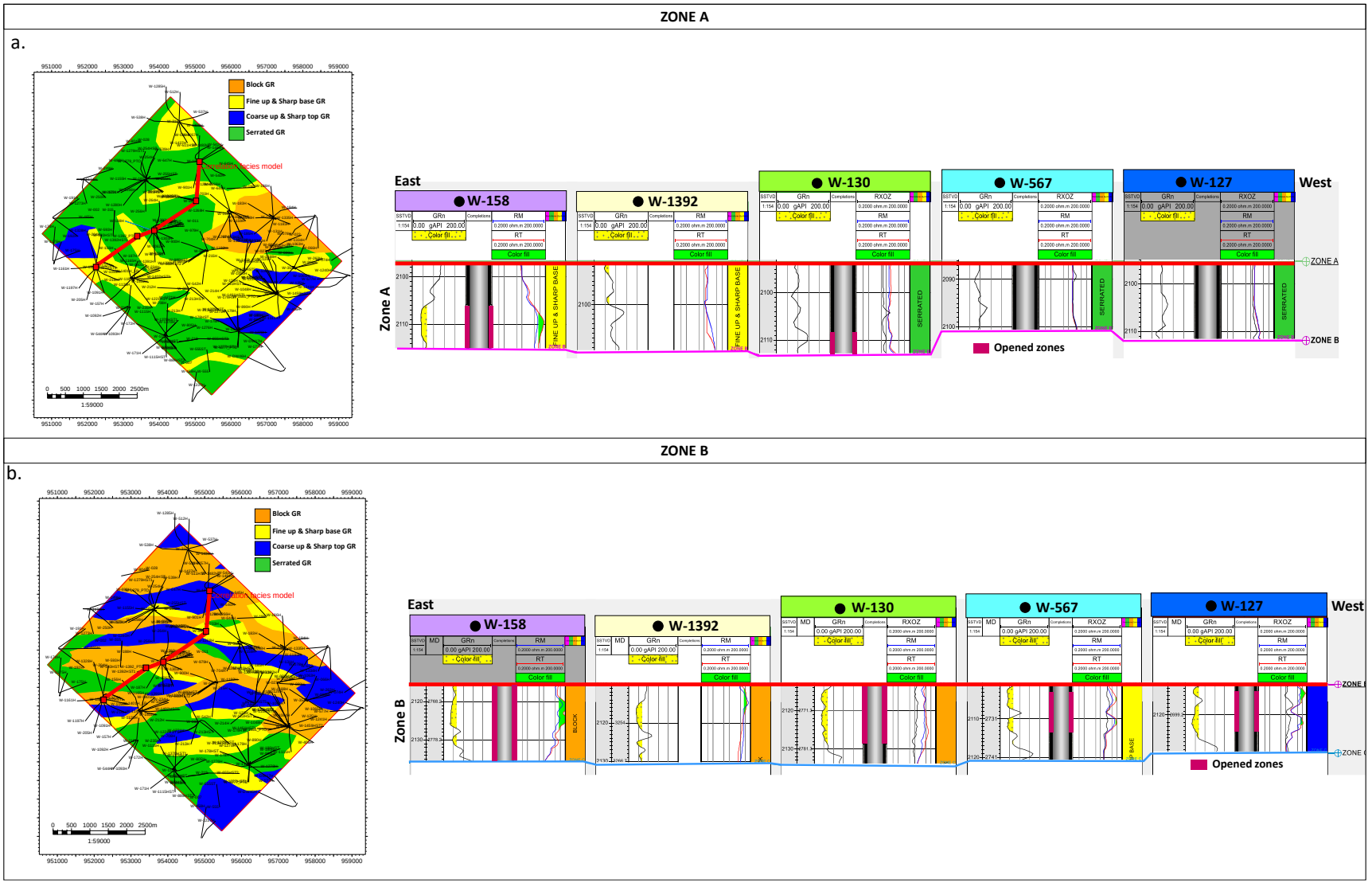

Figure 2-9. a. Electrofacies maps zone A and well correlation. b. Electrofacies maps zone B and well correlation.

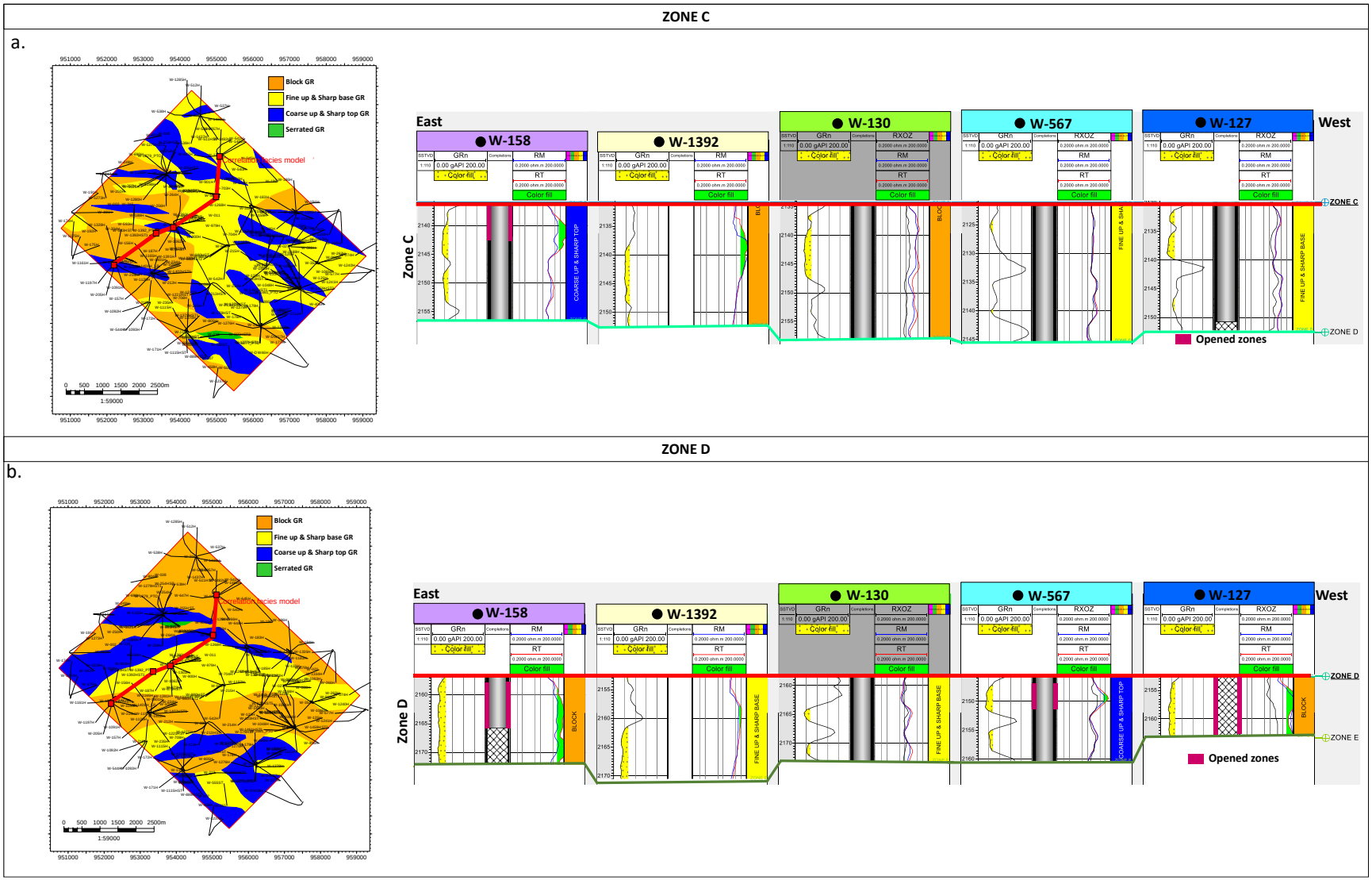

Figure 2-10. a. Electrofacies maps zone C and well correlation. b. Electrofacies maps zone D and well correlation.

2.5. PETROPHYSICAL MODEL

The petrophysical model was built by Ecopetrol S.A in 2017. The topics which are explained in this chapter were taken from technical reports presented by Ecopetrol S.A.

This model started using the lithotypes identified in the core description and the all petrophysical model are tie to four lithotypes. (Figure 2-11).

- **Lithotype 1 and 2**: are coarse to medium grain size sands. They are considered as reservoir rocks and their stain depends on the degree of bioturbation, sorting, and grain size (Figure 2-11).
- **Lithotype 3**: is associated to facies type silt, laminated sands, or clay matrix and bioturbated sands. Although those lithologies are sandstones, they do not have any hydrocarbon potential (Figure 2-11).
- **Lithotype 4:** are siltstone facies which include coaly siltstones, bioturbated siltstone and siltstones (Figure 2-11).

In the AOI has 36 vertical wells, which have a basic set of logs such as GR, spectral GR, SP[11], Neutron-Density, resistivity, sonic. Some of them have special logs as formation pressure, magnetic resonance, check shot, VSP[12] and sonic scanner etc. (Ecopetrol, 2017).

The horizontals and deviated well which are190 wells in total were logged by LWD[13] where only acquire GR and resistivity.

In this AOI, it is only two cores available, W-158 has basic and special analysis, while W-130 does not have those laboratory experiments because its poor core recovery. Nevertheless, this petrophysical model belongs to an extensive area bigger than the area of interest so it had more information to tie the model.

The petrophysical well log model extrapolated the lithotypes identified in the core to the logs. According to cores it was identified 12 types of deposits and they were grouped depending on the quality of reservoir.

[11] Spontaneous Potential. Continuous recording vs. depth of the electrical potential difference between a movable electrode in the borehole and a surface electrode

[12] Vertical Seismic Profile. is a technique of seismic measurements used for correlation with surface seismic data.

[13] Log While Drilling

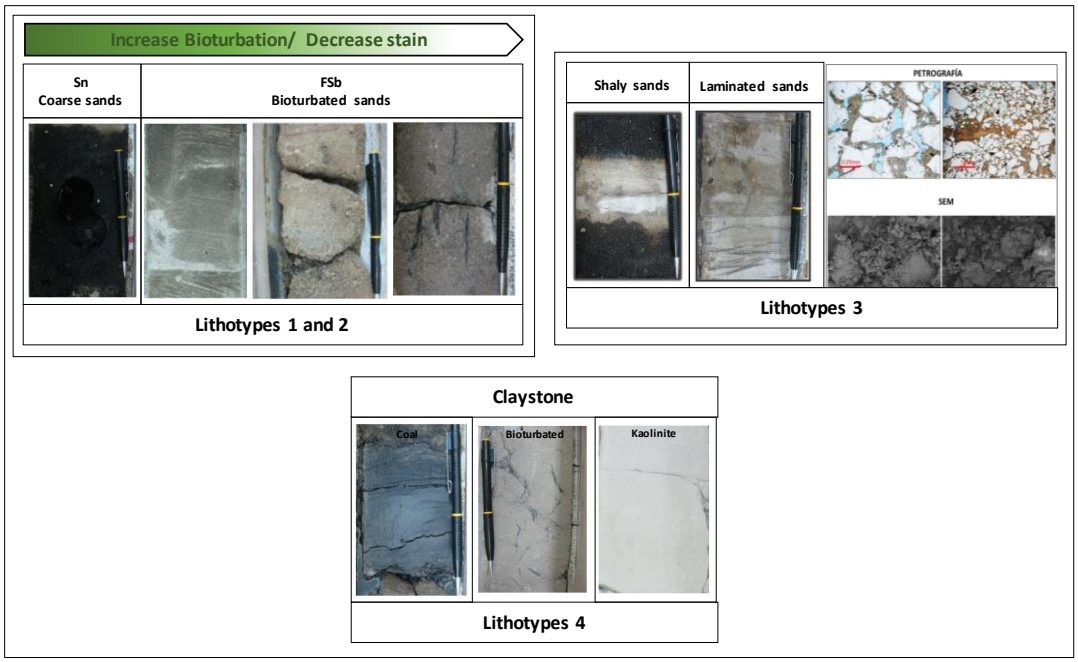

Figure 2-11. Lithotypes used in the petrophysical model.

2.5.1. Shale Volume Model

This area has very clean sandstones deposited in a fluvial environment with a good lateral continuity, so those clean rocks have very low values of shale volumen. This model was adjusted through the following equations with the following parameters (Ecopetrol, 2017).

$$VClayGR = \frac{\mathrm{GR}_{log} - GR_{Clean}}{GR_{Shale} - GR_{clean}} \qquad \textbf{Equation 2-1}$$

$$VclayDN = \frac{DEN_{log} - DEN_{mtx} + NEU_{log} * (DEN_{mtx} - DEN_{fl})}{DEN_{shale} - DEN_{mtx} + NEU_{shale} * (DEN_{mtx} - DEN_{fl})} \qquad \textbf{Equation 2-2}$$

Where:

GR_{log} : Gamma ray from logs.
GR_{clean} : Gamma ray clean (Sandstone).
GR_{Shale} : Gamma ray Shale.
DEN_{log} : Density from log.
DEN_{mtx} : Density from matrix.
DEN_{fl} : Density fluid.
NEU_{log} : Neutron from log.
NEU_{Shale} : Neutron Shale.

The shale volume model reproduces low values under 10% in the best rock lithotype 1 and 2. In the lithotype 3 moderate and high values of shale were obtained between 5 to 30%. The low shale volume values are associated to channel and bars facies, and the moderate to high are correlated to levee, overbanks, and abandoned channel facies among others (Ecopetrol, 2017).

2.5.2. Porosity Model

The effective and total porosity model was calculated using neutron and density logs. The following are the equations and parameters used.

$$PhiDEN = \frac{RhoM/Rholog}{RhoM-RhoFluid} \qquad \textbf{Equation 2-3}$$

$$PhiA = \frac{PhiDEN-PhiNEU}{2} \qquad \textbf{Equation 2-4}$$

Lithotype	Matrix density (gr/cc)	Fluid density (gr/cc)
1-2-3	2.64	1-1.1
4	2.65	

Table 5. Parameter value used to calculate porosity from neutron -density log.

Matrix density was gotten from laboratory measurements and it was compared to logs showing that the lithotype 1 and 2 have low variability. The density from shaly sands lithotype 3 was defined through core measures. Additionally, the magnetic resonance of W-158 shows high grade of mud invasion into the rock generating invasion of other material as well which means that this rock has high porosity.

2.5.3. Permeability Model

Permeability model was obtained through a combination of inverse gamma ray and multilineal regression of effective porosity and GR. The first model involves to make equivalent scales of minimum and maximum GR with minimum and maximum values of core permeability.

Inverse GR method overestimates the permeability in clean zones where pore throat radius is very small. Base on that permeability was calculated through a multilinear method of effective porosity and GR to compensate the effect of grain size (Ecopetrol, 2017). The following is the equation was obtained by multilinear method.

$$K_{Model} = 10^{(-1.622*(18.966*PHIE)+(0.021*GRn)} \qquad \textbf{Equation 2-5}$$

2.5.4. Rock Type Model from Logs

Pitman 50 was the method that better represented the pore throat in the reservoir. Permeability and porosity core data to 1000 psi were used. As a result of pore throat by capillary pressure (mercury and centrifuge) were used to identify 7 rock types (Figure 2-12).

The Pitman R50 equation used is presented below:

$$\log(R50) = -0.788 + 0.626 * \log(K)\ 1.205 * \log(PHIE) \qquad \textbf{Equation 2-6}$$

Rock type 2, 3 and 4 have an overlap on their pore throat radius (Figure 2-12a). but they have different irreducible water saturation (Figure 2-12b). That overlap is due to poor sorting and include fine grains which increase the irreducible water saturation.

The cutoff to classify rock types are presented in the following table:

Rock Type	1	2	3	4	5	6	7
R50	>=29	15-29	12-15	8.8-12	4-8.8	0.6-4	<=0.6

Table 6. Parameter R50 value used to calculate rock types.

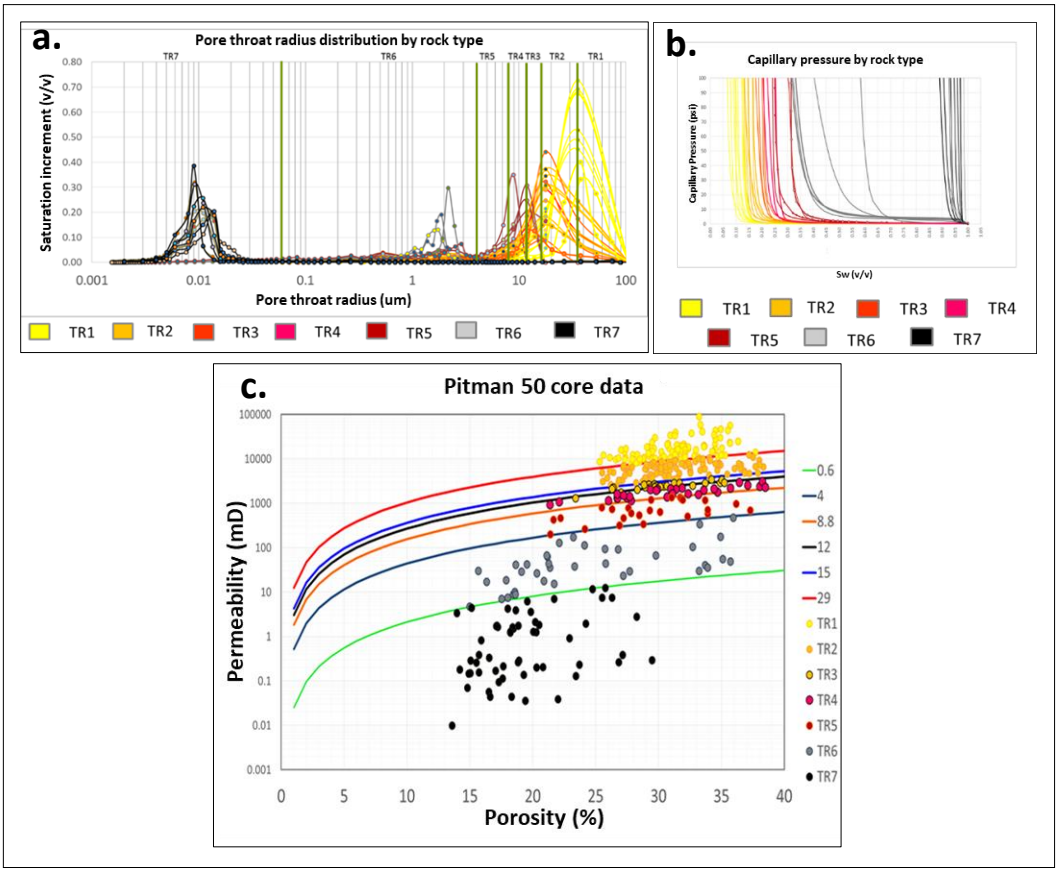

Figure 2-12. a. Pore throat radius by rock type, b. capillary pressure by rock type and c. Pitman R50 graph. (Modified from Ecopetrol, 2017)

Table 7 has the description of the main characteristics by rock type.

Rock Type	Lithology	Porosity (%)	Permeability (Darcies)	Irreducible wáter (%)
1	Quarzose sandstones. **Composed of:** 98% quartz – 2% clay (caolinite) **Sorting:** Poor **Grain size:** Conglomerate	>30	>8	8-13
2	Quarzose sandstones. **Composed of:** 98% quartz – 2% clay (caolinite) **Sorting:** Moderate **Grain size:** Conglomerate to medium	30	3-8	18-25
3-4	Quarzose sandstones. **Composed of:** 85% **-** 98% quartz – 2% - 15% clay (caolinite) and organic material. **Sorting:** Moderate - good. **Grain size:** Medium -fine	28-30	0.9-3	30
5-6	Quarzose sandstones with more portion of clay. **Composed of:** 30% - 60% clay (caolinite). **Sorting:** Moderate - good. **Grain size:** Fine – very fine	16-25	0.01-0.8	69-80
7	Claystone-quartz wacke. **Composed of:** 98% quartz - 60% - 97% clay. **Sorting:** Moderate - good. **Grain size:** Conglomerate.	18	0.0001-0.001	90

Table 7. Description about rock types characteristic. (Modified from Ecopetrol, 2017).

2.5.5. Water Saturation Model

The water saturation model selected for this field was a capillary pressure model. This model defines the water saturation base on height function from the free water level.

Base on capillary pressure from centrifuge and J function method it was built the water saturation model. J function has inputs like porosity, permeability, capillary pressure. The water saturation was defined as a J function correlation by each rock type.

In some cases where water saturation model was optimistic the permeability was reduced and that levels were classified as rock type 5-6 to generate 100 % water saturation (Ecopetrol, 2017).

2.6. RESERVOIR ENGINEERING ASPECTS

2.6.1. Reservoir Pressure

Reservoir Pressure (Pres) has been stablished from MDT, PTA and SBHP data as shown in the Figure 2-13a. Reservoir pressure is between 625 to 1075 psia in the AOI. The lowest pressure area is in the southern part (red color Figure 2-13a).

2.6.2. Fluid Properties

The oil found in this area is classified as heavy oil based on its fluid properties (Table 8). According to PVT[14] taken in AOI, the fluids have low GOR, low bubble pressure, low volumetric factor, low API, and high viscosities. The oil viscosity shows an important variation observed in Figure 2-13b which shows the viscosity increment towards east.

Parameter	ID	Value	Units
Water Viscosity	μ_w	0.46	Cp
Oil Formation Factor	Bo	1.02	Rb/Stb
Oil Viscocity	μ_o	160-360	Cp
Temperature	T	145	°F
Bubble Pressure	Bp	80-165	Psia
Gas Oil Relation	GOR	5-14	(Scf/Stb)
Specific Gravity		11-14	°API

Table 8. Main fluid properties.

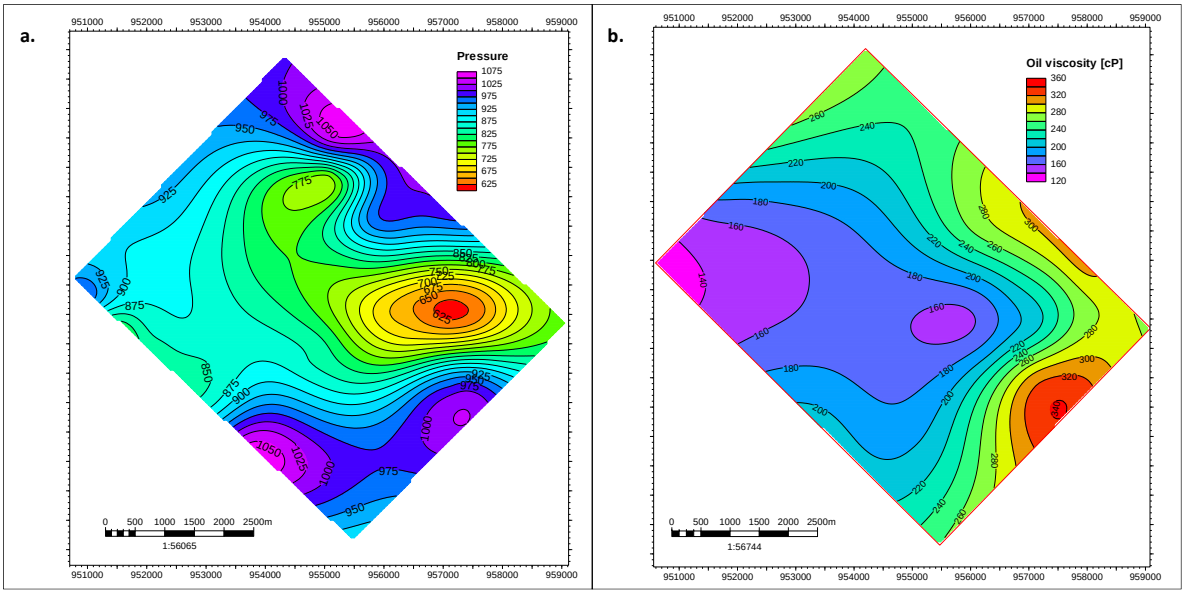

Figure 2-13. a. Reservoir pressure map. b. Oil viscosity map.

2.6.3. Laboratory Water – Oil Relative Permeabilities

The following figures show the available relative permeabilities per rock type (TR). Water oil relative permeabilities have different oil viscosities and this helped to correlate their end points with oil viscosity where information was not available.

[14] PVT: Pressure- Volume and Temperature. PVT is a common abbreviation in petroleum engineering to account for tests and fluid properties that changes when the pressure, volume and temperature are changed. For example, how the oil viscosity changes with temperature.

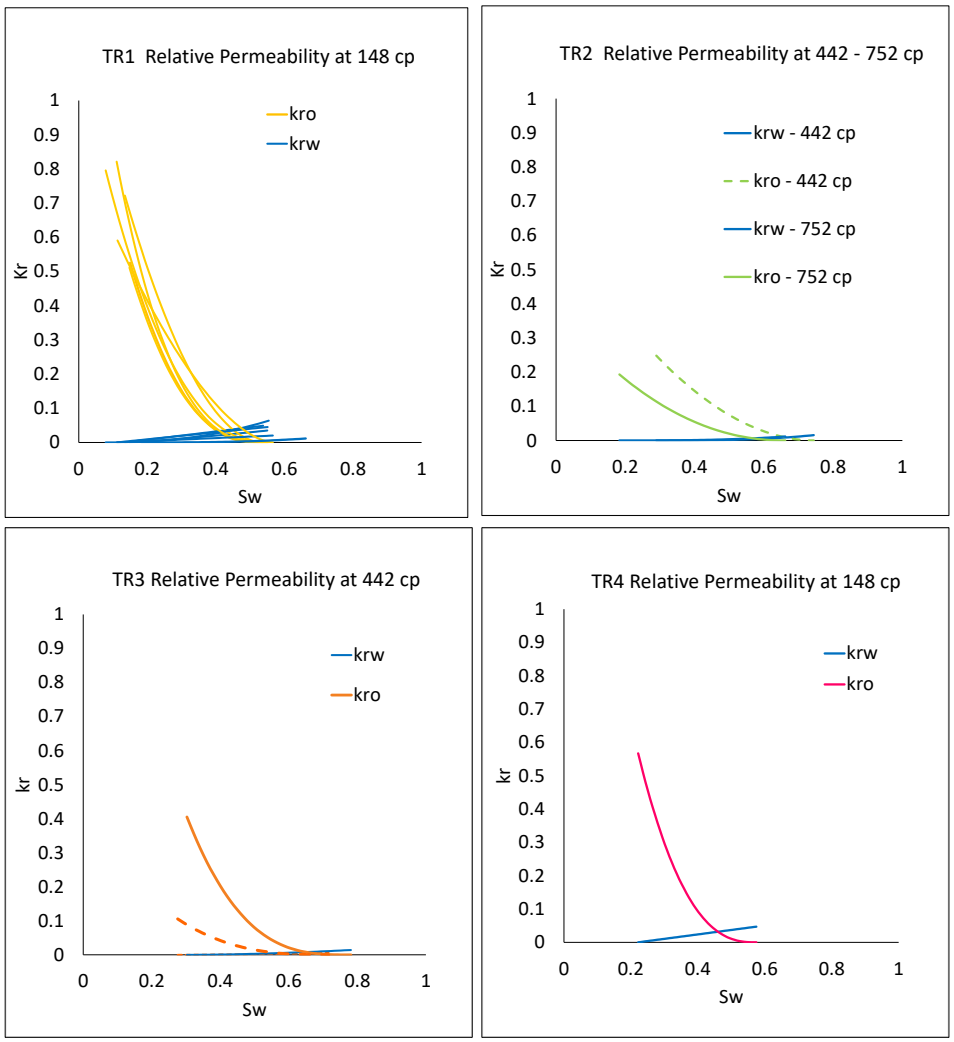

Figure 2-14. Relative permeability curves by rock type.

The table below summarized the end points per Rock Type, some values were filtered as they were highly affected by laboratory limitations.

RT	Porosity %	Air perm	Oil Viscosity (cp)	Swirr	Sorw	kro@swi kair ref	no
1	30.30	8913.00	148	0.150		0.820	
1	27.20	7350.70	148	0.148		0.790	
2	30.00	6230.00	752	0.183	0.338	0.193	2.860
2	29.90	6230.00	442	0.273	0.255	0.248	2.579
3	31.60	3282.00	442	0.275	0.284	0.105	2.760
3	30.00	6230.00	442	0.303	0.219	0.405	3.050
4	26.80	1681.10	148	0.222		0.567	
6	21.2	77.61	148	0.44	0.425	0.030	

Table 9. Laboratory relative permeability end-points.

3. METHODOLOGY AND WORKFLOW

This investigation is based on building a robust static model for a heavy oil field. Three main challenges arise: the first is about facies modelling and its relationship with geostatistical modelling approaches and the uncertainty in the facies distribution. The second challenge is how to estimate the oil rate knowing that the oil relative permeability is not conventional and that it is required to develop a method to deal with that complexity, and third is how to integrate the static modelling and the reservoir engineering properly to calculate sweet spot, to solve these challenges, it was developed the following methodology and workflow (Figure 3-1).

3.1. LITERATURE REVIEW

This step has two main goals. The first goal is to review and find the latest existing literature on geostatistical facies modelling, facies impact on oil reservoirs modelling and relative permeabilities correlations.

The second goal is to get academic, methodological, and experimental support through official documents such as thesis, journal articles and books.

3.2. DATA PREPARATION

This work is oriented to build a 3D static model focused on the facies distribution and its impact on oil rate production, so in that context the geological, petrophysical, and engineering information needed is very specific and must be selected with careful quality control to get reliable results.

As reference, this project has 226 wells in total, including vertical, deviated, and horizontal wells.

3.2.1. Information Gathering and Inventory

The data collected has different sources and scales. The static model integrates a large amount of information from various disciplines such as Geophysics, Stratigraphy, Sedimentology, Petrophysics, and Petroleum Engineering.

In this phase, the basic data gathered comes from well information such as coordinates, elevation references, directional surveys, well tops, well logs, petrophysical logs, well completions, pressures, oil viscosities, relative permeability curves and pressure build ups. The incorporation of facies map images that come from the sedimentological model. The data set and facies images were provided by Ecopetrol S.A.

3.2.2. Data Quality Control.

The data described in the previous step must be checked to optimize the time during the modelling phase and eliminate inconsistencies. The most important reason to do a good quality control is to guarantee coherence and satisfactory results. This step is commonly overlooked, especially the QAQC related to flow capacity prediction of the static model where the petrophysical model, static model and pressure transient analysis converge.

Input data quality control is done by a statistical analysis and a visual inspection. Histograms and cross-plots allow to capture of null data, anomalous values, errors, distributions, outliers etc. Isochore and well distribution maps are used to identify inconsistencies in elevations datum, tops, and coordinates.

3.2.3. Lithofacies Inputs

Digitalized Electrofacies Maps: Digitalizing electrofacies maps and converting them into a 3D grid allows for the building of discrete logs by well.

Lithofacies Log Generation: This is a special item in the methodology because lithofacies is a discrete log which must be created from other logs such as normalized gamma ray and electrofacies.

Lithofacies log results are checked through permeability and porosity cross-plots to perform a quality control and to find a correlation between petrophysical properties and lithofacies. This process shows how to link petrophysical and geological models.

3.3. 3D STATIC MODELLING

At this stage it is presented the basic steps to build the static model where the geostatistical techniques are used combined with the uncertainty workflow proposed in this study.

3.3.1. Building a 3D grid:

Define the cell size and number of layers for the 3D model. These parameters depend on the heterogeneity and computational capacity.

Cell Size: The grid size is selected based on heterogeneity, horizontal wells coverage and CPU[15] time. The grid size selected was 20*20 in IJ and 1 foot in K direction respectively, and this grid is oriented North west direction almost parallel to flow channels.

Number of layers: The number of layers is defined by several iterations to find which layer thickness is the best option to model. The following is the procedure to define the number of layers was used:

- Calculate gross thickness by zone and by well, covering all zones to be modeled.
- Divide the well gross thickness obtained by the layer thickness selected (several scenarios are considered here). Layer thickness is selected according to lamination thickness (vertical heterogeneity). The result of this operation yields the number of layers per well and per zone.
- Calculate the mean of the number of layers per zone.
- Run the layering model per zone with the acquired mean value and upscale the facies log for each scenario considered. This step is repeated until the minimum difference between the upscaled model and the lithofacies log is found.

The number of layers selected include those which exhibit the same statistical behavior and have similar values to the raw data. Achieving these conditions is produced an optimal number of layers.

[15] CPU time is a common term use in reservoir simulation to quantify the time in hours of days that a model takes to run the history and prediction. It is desired to have a model that take no more than a couple of hours to run in order to identify possible changes either to adjust it from history match of to generate multiple options in prediction mode.

In this study the average cell height is 1 foot in order to capture vertical heterogeneity presented in fluvial and transitional environments.

3.3.2. 3D Lithofacies Modelling

This model was built within the stratigraphic and structural framework captured into the grid generated. There are many options to perform lithofacies modelling. Nevertheless, in this study only one method was strong enough to model fluvial environments and able to reproduce the heterogeneity and bodies connectivity.

The methods used were: Sequential indicator simulation (SIS) (one using data from sedimentological maps and other using sedimentological geomorphology), truncated gaussian simulation (TGS), and multiple point simulation (MPS). SIS and TGS are commonly used to model facies; they are supported by variograms and can integrate various data types and MPS characterizes the spatial structure by multiple data points through training images.

3.3.3. Petrophysical Modelling

In this step, petrophysical variables are distributed across the 3D model using the lithofacies model as a constraint, giving a geological and petrophysical consistency to the static model.

Shale volume, porosity and permeability will be modeled using the sequential gaussian simulation method, and permeability is also be modeled using the collocated-kriging method in order to keep the linear correlation between them.

Net to gross (NTG) was calculated using a normalized shale volume. Water saturation was calculated into the grid based on a height model (capillary model).

3.3.4. Volumetric Calculation

Volumetric calculation is the common final step when building a static model as it is related to the material balance commonly used in reservoir engineering.

In this study, the number of volumetric scenarios depend on the number of models generated and will be used for further analysis in the uncertainty section.

3.3.5. Lithofacies Uncertainty Analysis

To evaluate the uncertainty was proposed a workflow where multiple realization of facies scenarios are run into a training and base cases for each geostatistical facies technique. These realizations were done through Monte Carlo analysis. It was selected from the last 300 realization (reference model) only five percentiles P10, P35, P50, P75 and P90 which represent the distribution.

3.4. RESERVOIR ENGINEERING CALCULATIONS

Reservoir Engineering calculation is a special step proposed in this project. Usually static and dynamic models are built apart without any connection. The aim of this step is to guarantee and smooth transition between static and dynamic model as it guarantees that the initial point (the initial oil rate) is calibrated as close as possible to the observed data, therefore it is expected that the history match in the dynamic model stage can reduce its CPU time.

The initial oil rate is estimated cell by cell in this study. It was assumed that the solution of diffusivity equation under pseudo steady state conditions can give close results to those use by a reservoir simulation model.

Additionally, since this work is going to be done for heavy oil fluids, it was necessary to perform an additional analysis on the oil relative permeability. The relative permeability is commonly assumed that only depends on saturation, but for heavy oil reservoirs the relative permeability is also function of oil viscosity. Therefore, it was proposed a methodology[16] to correct this oil relative permeability as function of the oil viscosity.

3.4.1. Pressure Transient Analysis

Available Pressure build ups (PBU) are interpreted to obtain flow capacity (Kh), formation damage (skin), and productivity index (PI), among other variables. These parameters were used for the oil rate production calculation and for quality control of the Kh coming from the static model.

It is worth noting that the higher the number of good pressure transient analysis (PTA[17]), the higher the accuracy of the flow capacity (Kh) match across the model will be.

3.4.2. Flow Capacity Match

The flow capacity (Kh) obtained from the PBU is used to calibrate the static model Kh and the oil relative permeabilities. More iterations are required when less data is available.

3.4.3. Productivity Index.

At this stage, the Kh from the static model and oil relative permeabilities are adjusted using PTA information. The next step is to estimate the productivity index (PI) for all the wells.

The purpose of using the PI is to estimate the bottom hole flowing pressure (Pwf) in wells where PTA information is not available Notice, that the Pwf is a key parameter to estimate the oil rate.

[16] Notice that the methodology proposed in this study is for heavy oil reservoirs but it can easily be extrapolated to other fields where the relative permeability depends on other parameters.

[17] PTA: Pressure Transient Analysis, this is the generic term to refer to different pressure transient analysis test such as Draw Down (DD) and pressure build ups (PBU). In this study it will be use PBU interpretations to estimate the flow capacity of the well.

3.4.4. Calculation of Initial Oil Rate into Geological grid

Once the static data (Kh) and engineering data (PI and oil relative permeability) are calibrated, the initial oil rate (Qo) can be calculated into the geological grid. Each grid cell will have a value of Qo and the calculation will be compared with the measured initial oil rate production from vertical wells accounting for the perforated interval in order to corroborate the predictability of the model.

3.5. RESULTS AND CONCLUSIONS

The results are presented using histograms, grid images from specific layers, and cross-plots. All these graphic elements will compare the initial oil rate for different lithofacies as well as other possible comparisons.

The idea is to compare visual dissimilarities and similarities among all results obtained to identify which zones have similar results across all scenarios. In other words, the uncertainty analysis helps to identify facies characteristics where the majority number of realizations for different lithofacies repeatedly coincide. This hypothesis is the same for the oil rate.

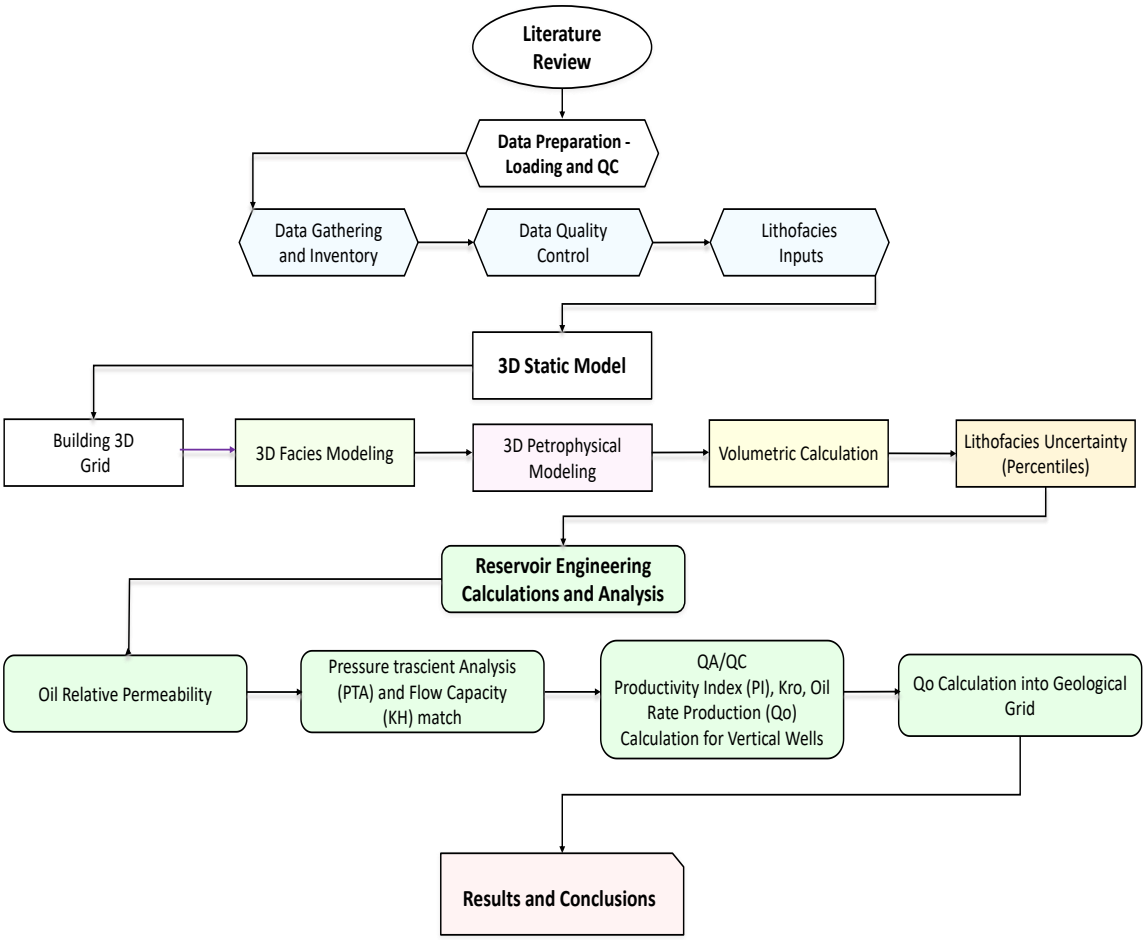

Figure 3-1. General workflow - Methodology.